ANNUAL REPORT

1979

R.J. Van de Graaff Laboratory

Utrecht The Netherlands

ANNUAL REPORT

1979

Physics Department
University of Utrecht,
P.O. Box 80.000,
3508 TA UTRECHT
The Netherlands

Printed by Elinkwijk B.V., Utrecht
July 1980

PREFACE

A few years ago, one of the major physics journals introduced a page charge. In order to enable the reader, and in particular the writer, to calcualte the costs of publishing an article, a polynominal was presented. Besides the obvious term in n, where n is the number of pages of the article, it contained additional terms in n^2 and n^3, both with non-negligible coefficients. For reasons unknown to me, the journal dropped the formula within a few months, and luckily also the page charge. The point of the short-lived polynominal, however, is clear: for the survival of physics publications conciseness is imperative.

The authors of the present annual report have not been compelled to obviate n^2 or n^3 terms, but they were kindly invited to write their contributions as concisely as is compatible with clarity. Consequently it is impossible to summarize the report on this one page. By mentioning a few trends and highlights, this preface hopefully stimulates reading of the following pages.

A comparison with previous reports in this series indicates that:

- The number of fp-shell nuclei studied is increasing; this field complements the research on sd-shell nuclei, Utrecht territory by tradition. Information on these slightly heavier nuclei has been obtained with the tandem accelerator, the 4 MV Van de Graaff and with the high-flux reactor in Petten. It is not by accident that the center-of-gravity of the theoretical calculations is simultaneously shifting towards the fp-shell.
- The number of undergraduate students in our nuclear physics department is continuously growing.
- The number of publications is this year relatively low. We expect this to be a statistical fluctuation, without implying that the publication of scientific papers is a purely statistical process; this expectation is supported by the number of papers presently in press.

During the year reported here, quite some attention has been devoted to the design, development or installation of new apparatus:

- A Compton-suppression spectrometer for γ-γ coincidence experiments has been designed which combines a large solid angle with excellent Compton suppression. A gain as large as an order of magnitude seems feasible.
- Two new computers have been installed for data collection.
- An analyzer and detectors for radiocarbon dating with the tandem accelerator are under construction.
- The workable range of the 4 MV Van de Graaff was extended to lower energies by the installation of a shorting rod assembly. No news, however, was received during 1979 on the planned extension of the facilities to higher energies.

As usual precision spectroscopy is the continuous thread that runs through our annual report. A few examples are:

- Nuclear spins, unambiguously determined (shunning model-dependent arguments). This refers to both the high spins deduced from heavy-ion work and the lower spins found in proton and neutron capture experiments.
- Nuclear lifetimes, determined with a precision of a few percent through the careful consideration of the slowing-down process of ions in solids.
- The output from the g-factory.
- The measurement of the energy of a 6 MeV γ-transition with a precision of better than 10 ppm, stimulated by a highly appreciated IUPAP collaboration.

Monique de la Bey expertly typed this report.

Pieter Endt did most of the editing, until he got absorbed by other duties, mainly in the reviewing field. The subsequent reshuffling of the editorial responsibilities unfortunately caused some delay. It should be stated, however, that writing reviews is also a respectable business. At least it is useful, as was pointed out by the Institute for Scientific Information in Chicago. In a search for frequently quoted physics articles, it identified a previous edition of our $A = 21$-44 review articles as a "Citation Classic".

Cor van der Leun

SCIENTIFIC STAF

Prof. P.M. Endt
Dr. G.A.P. Engelbertink
Prof. A.M. Hoogenboom
Dr. R. Kamermans
Prof. C. van der Leun

Prof. P.J. Brussaard
Prof. P.W.M. Glaudemans

VISITING SCIENTISTS

Dr. M. Adachi (Tokyo, Japan)
Prof. R. Kalish (Haifa, Israel)
Prof. H. Lancman (City University, New York, USA)
Dr. J.J.A. Smit (Potchefstroom, South Africa)

POST-DOCTORALS

Dr. C. Alderliesten
Dr. K. van der Borg
Dr. G.A. Timmer

GRADUATE STUDENTS

H.J.M. Aarts
H.F.R. Arciszewski
E.L. Bakkum
J.R. Balder
A. Becker
Ginevra Delfini
R.J. Elsenaar
A.G.M. van Hees
A. Holthuizen
B.C. Metsch
R.B.M. Mooy
G.J.L. Nooren
C.J. van der Poel
A.J. Rutten
J.F.A.G. Ruyl
D.E.C. Scherpenzeel
A. Tielens
R. Vennink (Ph.D. 1979)
J.J.M. Verbaarschot
D. Zwarts

SECRETARIAL STAFF

Monique de la Bey
Everdina M. Bos

UNDERGRADUATE STUDENTS

P.F.A. Alkemade
P.J. van Baal
Mrs. S. Bazna-Lucardie
F.M. Bloemen

UNDERGRADUATE STUDENTS (CONT.)

R.C.H. Broers
A. Buys
D. Dijkkamp
C. Dommisse
A.J.H. Donné
C.P.M. van Engelen
E.M. van Gasteren
O.A. van Herwaarden
T.A.M. Heunks
T.L.M. Hoogenboom
J. Hop
P.M.J. Hoppenbrouwers
J.C.K. Kock
J. Kroon
D.J. van Meeuwen
S. van der Meij
J.A. van Nie
J.H. Nokkert
A.P. Riethoff
A.P. Slok
G.N.A. van Veen
F.C.M. Verhagen
H. van der Vlist
F. Zijderhand

TECHNICAL STAFF

Dr. A. Vermeer
R.J. Elsenaar
P. de Wit
D. Balke
A. van den Brink
Wendy Ficker
J.P. van der Fluit
S.A. Gerrits
A.P. de Haas
F.A. Hoppe
W.P. Ingenegeren
H.J.H. Kersemaekers
J.J. Langerak
G.W.M. van der Mark
A.J. Michielsen
C.J. Oskamp
R. Riemens (apprentice)
W. Smit
J. Sodaar
B.A. Strasters
A.J. Veenenbos
Ph.E.P. van der Vliet
R. Vos (apprentice)
H. de Vries
H. Woltjes (apprentice)
N.A. van Zwol

CONTENTS

1.1. Nuclear structure investigations with heavy ions

H.J.M. Aarts, H.F.R. Arciszewski, G.A.P. Engelbertink, E.M. van Gasteren, T.L.M. Hoogenboom, D.J. van Meeuwen, C.J. van der Poel, D.E.C. Scherpenzeel and F.C.M. Verhagen

HIGH-SPIN STATES IN LIGHT NUCLEI

In the past year the Monte Carlo design calculations for a Compton-suppression spectrometer (CSS) with large solid angle have been completed. The present CSS with the small solid angle of 7.5 msr is very suitable (see e.q. next section) for the measurement of singles spectra and angular distributions, because in such one-detector experiments the (advantageously) small solid angle can be compensated for by the use of a higher beam intensity.

In the present γ-γ coincidence experiments, however, the CSS is typically combined with three or four (gating) Ge(Li) detectors of about 600 msr solid angle each. In this poorly matched situation, the maximum coincidence count rate between the CSS and a gating Ge(Li) is then determined by the maximum singles count rate of the Ge(Li) detector, which with present electronics amounts to about 40 kHz.

The Monte Carlo calculations show that it is possible to construct a CSS with roughly the same Compton suppression as the present spectrometer but with an efficiency which is about a factor of ten larger. The new 120 msr solid-angle CSS, especially suited for γ-γ coincidence measurements, will be installed in February 1980.

Properties of yrast levels in ^{34}Cl, ^{44}Ca and ^{59}Ni have been investigated. High-spin levels of these nuclei are populated in the reactions ^{24}Mg(^{12}C,pnγ)^{34}Cl, ^{28}Si(^{18}O,2pγ)^{44}Ca and ^{46}Ti(^{16}O,2pnγ)^{59}Ni at bombarding energies of 30-45 MeV. Some results specific for ^{34}Cl are discussed below.

In the ^{24}Mg + ^{12}C reaction, 1935 and 2489 keV γ-rays are strongly coincident with the 491 keV decay γ-ray from the lowest $J^{\pi} = 7^{+}$ level at $E_x = 5.32$ MeV. Since the two γ-rays do not stem from the known decay of lower-lying levels, they originate from levels with $E_x > 7.2$ MeV. Further information is obtained from the ^{31}P(α,nγ)^{34}Cl reaction. Figure 1 gives results from this reaction and shows spectra taken at bombarding energies of $E_\alpha = 16.33$, 15.70 and 14.90 MeV in coincidence with the 491 keV γ-ray. The bombarding energies correspond with the thresholds A, B and C indicated at the righthand side of the figure. Since no low-energy γ-rays are observed, measurement C implies that the 1935 keV γ-ray originates from a level at 7.25 MeV. Measurement B similarly shows that the 2489 keV γ-ray stems from $E_x = 7.80$ MeV. The absence of the 2489 keV peak in measurement C is consistent with this level scheme. These two new levels presumably have spins higher than $J = 7$.

A similar measurement as B but at $\theta_\gamma = 0^{\circ}$ and with a 110 μg/cm^2 ^{31}P target on thick gold yields the lifetimes of these levels because the threshold is low enough to neglect delayed feeding. The results are τ_m(7.80 MeV) = 100 ± 70 fs and τ_m(7.25 MeV) = 200 ± 70 fs.

Angular distributions, measured in the ^{24}Mg + ^{12}C reaction, and strength considerations are in this particular case sufficient to yield definite spin-parity assignments of J^{π}(4.74 MeV) =

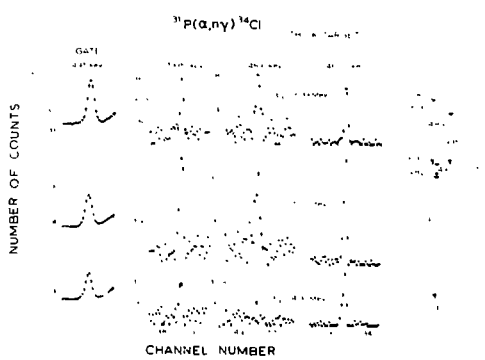

Fig. 1. Spectra of γ-rays from the $^{31}P(\alpha,n\gamma)^{34}Cl$ reaction taken at beam energies of $E_\alpha = 16.33$, 15.70 and 14.90 MeV in coincidence with the 491 keV γ-ray. The bombarding energies correspond with the thresholds A, B and C indicated at the right-hand side of the figure.

6^-, $J^\pi(4.82\ \text{MeV}) = 5^+$ and $J^\pi(5.32\ \text{MeV}) = 7^+$. Fig. 2 shows the latter result. The absence of side-feeding to the 4.82 MeV level in this case gives a strong coupling between the alignment parameters of the 5.32 and 4.82 MeV levels. This coupling combined with an accurate measurement of the A_4 coefficients of the 491 and 4677 keV angular distributions is sufficient to eliminate the (competing) $J^\pi = 5^+$ possibility. Angular distributions for the 1935 and 2489 keV γ-rays are lacking at present because in singles the 1935 keV peak is part of a triplet and the 2489 keV peak is very weak.

If the yrast 7^+ state at 5.32 MeV is interpreted as an $(f_{7/2})^2_{7^+}$ pair coupled to the ^{32}S ground state then the coupling of the pair to the ^{32}S first excited 2^+ state at 2.2 MeV would give rise to a 9^+ level at about 7.5 MeV excitation energy. It is possible that one of the new levels at 7.25 and 7.80 MeV discussed above is the ^{34}Cl yrast 9^+ state. With the assumption of E2 character, the strength of the 7.80 → 5.32 MeV transition would amount to 7 W.u. and the 7.25 → 5.32 MeV transition to 24 W.u. The $^{32}S(2^+_1 \rightarrow 0^+)$ core transition has an E2 strength of 9 W.u.

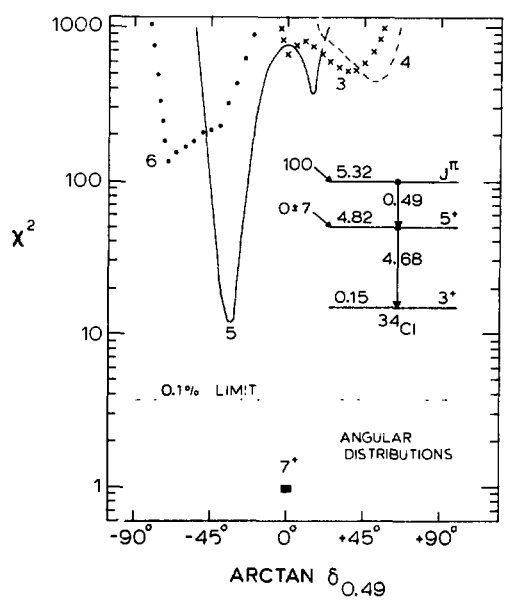

Fig. 2. Results of the least-squares analysis of the angular distributions of the 5.32 → 4.82 MeV and 4.82 → 0.15 MeV transitions of ^{34}Cl. The absence of side feeding to the 4.82 MeV level in this case gives a strong coupling between the alignment parameters of the 5.32 and 4.82 MeV levels.

IMPROVEMENT OF THE PERFORMANCE OF A COMPTON-SUPPRESSION SPECTROMETER

The performance of a CSS is, apart from the dimensions of the anticoincidence shield, mainly determined by the quality of the central detector and the amount of non-detecting material between the central detector and the surrounding shield. Transmissionwise, the dead Ge layer around the central Ge crystal is the main source of non-detecting material and its effect on the background is investigated by comparing CSS performance for a conventional Ge(Li) crystal with 1.0 mm dead layer and a high-purity germanium (HPGe) crystal with a 0.2 mm thick Li-diffused outer contact. The properties of the two detectors are given in table 1. The thickness of the dead layer of the HPGe detector was obtained from the observed area ratio of the (79.6 + 81.0) keV complex and the 53.1 keV γ-rays from a collimated ^{133}Ba source, in the way as shown in fig. 3.

The effect of a continuous variation of the thickness of the dead layer has been studied before [1] by means of Monte Carlo calculations. For a reduction of the dead layer from 1.0 to 0.22 mm, these calculations predict for ^{60}Co an improvement of about 35 % for the overall Compton suppression.

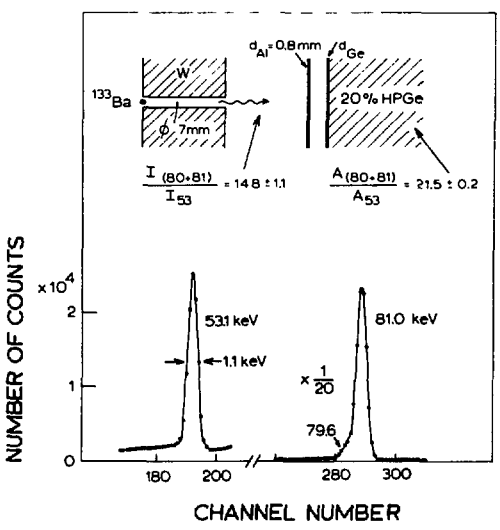

Fig. 3. Method to measure the dead-layer thickness of a Ge detector. The method is based on the difference in transmission of the dead layer for the (80+81) keV complex and the 53 keV γ-ray of a ^{133}Ba source. For the present HPGe detector the area amounts to $A_{(80+81)}/A_{53} = 21.5 \pm 0.2$. The lower part gives the thickness of the dead layer as a function of the measured area ratio.

With the HPGe crystal as central detector a ^{60}Co spectrum has been recorded with a PDP 11/40 computer. The HPGe-NaI anti-coincidence pulse is used to gate two ADC's, such that two spectra, one coincident (denoted as CO) and one anti-coincident (denoted as ACO) with the NaI pulse, are recorded simultaneously. The sum of the two recorded spectra (CO + ACO) gives the result without Compton suppression, i.e. the normal HPGe spectrum. The ratio between the number of counts in spectrum (CO + ACO) and spectrum ACO represents the Compton suppression as a function of energy. It is shown in the upper part of fig. 4. The average Compton supression between 100 and 1100 keV amounts to 11.2.

The Compton suppression for ^{60}Co with the 1.0 mm dead layer Ge(Li) is obtained similarly as described above. The result is shown in the middle part of fig. 4. The average Compton suppression between 100 and 1100 keV is now 3.4.

The lower part of fig. 4 gives the ratio of the two Compton suppressions and thus shows the improvement in performance of the spectrometer as a function of energy. The improvement is especially notable for the high-background region around the Compton edges (800 - 1150 keV), i.e. the energy region corresponding to the escape of Compton-scattered photons of low energy from the central detector. Reduction of the dead layer surrounding the central detector makes it more transparant for these low-energy γ-rays, which can now more easily reach the surrounding shield to produce a veto signal. The average improvement for 100 - 1100 keV is 32 % in good agreement with the Monte Carlo prediction of 35 %.

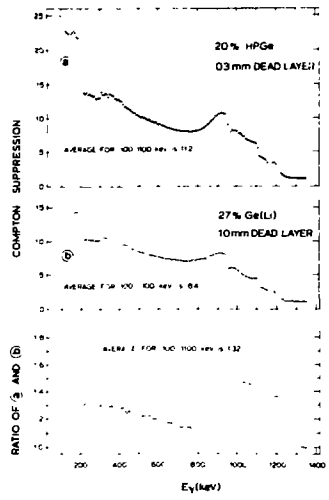

Fig. 4. Comparison of the ^{60}Co Compton suppression for the 1.0 mm dead layer Ge(Li) and the 0.2 mm dead layer HPGe crystal as central detector. The differences for E_γ < 200 keV between the top and the middle curve are probably due to different timing properties.

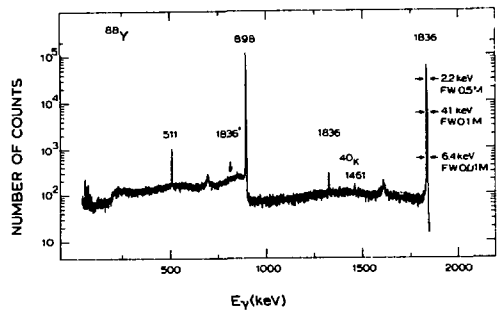

Fig. 5. Compton-suppressed spectrum of a ^{88}Y source.

TABLE 1. Properties of the two detectors used as central crystal in a CSS.

Manufacturer	Philips Nederland BV	Harshaw Chemie BV Holland
Type	Ge(Li)	HPGe
Active volume	126 cm^3	90 cm^3
Core	inactive germanium	hollow
Thickness dead layer	1.0 mm	0.22 mm
Thickness Al-cap: front	0.5 mm	0.5 mm
side	0.5 mm	0.8 mm
Operating Voltage	4500 V	3000 V
Efficiency	27%	20%
FWHM (1.33 MeV, ^{60}Co)	2.4 keV	1.9 keV
Peak-to-Compton ratio	46	50

Fig. 5 gives the spectrum from a ^{88}Y source taken with the present set-up. The peak-to-Compton ratio for the 1836 keV peak is 650, i.e. the residual Compton background is lower by almost three orders of magnitude. The sum of the area's of the 898 and 1836 keV peaks amounts to 62 % of the total number of registered counts.

Fig. 6 shows the low-energy part (E_γ < 2 MeV) of a singles γ-ray spectrum of the heavy-ion reaction $^{24}Mg + ^{16}O$ at $E(^{16}O)$ = 45 MeV and $\theta_\gamma = 90^o$. The upper spectrum is without the NaI veto and the lower one is the Compton-suppressed spectrum. The background suppression varies from about 7 to 12. This spectrum shows the advantage of a CSS for in-beam γ-ray spectroscopy. Weak and hardly visible peaks in the upper spectrum stand out clearly in the lower spectrum, see e.g. the 350 and 1400 keV regions.

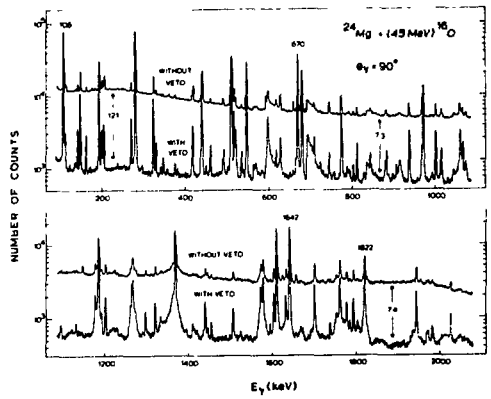

Fig. 6. Suppressed and non-suppressed γ-ray spectrum observed with the CSS at $\theta_\gamma = 90^o$ in the bombardment of a 320 μg/cm², 99.94 % enriched, ^{24}Mg target on thick Au with a 45 MeV, 100 nA, $^{16}O^{6+}$ beam after 5 h measuring time.

TABLE 2.

Summary of present coincident high-velocity DSA results

Nucleus	E_x (MeV)	E_γ (keV)	S(0) (%)	TiD (μg/cm²)	Slowing down material [a]	τ_m (fs)	χ^2	Statistical error (fs)	Adopted error [b] (fs)	Adopted τ_m [c] (fs)
^{28}Si	1.78	1778	5.02	[d]	Ag	683	1.5	9	35	688 ± 26
			5.02	[d]	Cu	695	1.2	17	39	
^{29}Si	1.27	1273	4.86	38	Au	429	1.4	5	22	420 ± 15
			4.77	190	Au	432	0.9	3	22	
			4.76	180	Cu	410	1.6	4	21	
			5.01	190	Mg	[e]	1.5	3	22	
	2.03	2028	4.84	38	Au	458	1.3	5	23	442 ± 14
			4.78	190	Au	437	1.2	4	22	
			4.71	180	Cu	434	1.1	6	23	
			4.86	190	Mg	449	1.6	7	24	
	2.43	2425	4.75	38	Au	26.6	1.8	1.0	1.6	26.6 ± 1.6
	3.07	1794	4.76	38	Au	45.8	2.0	1.3	2.6	46 ± 3
	3.62	1595	4.82	190	Mg	3770	1.1	70	200	3740 ± 190
		2028	4.73	190	Mg	3720	1.6	50	190	
^{30}Si	2.24	2235	4.91	[f]	Mg	358	1.2	3	18	358 ± 18

[a] For Au, Ag and Cu the experimental stopping powers of Forster et al. [4b] are used. The Mg data are analysed with S_{29}, see text.

[b] Quadratic addition of statistical error and 5% stopping power error.

[c] See text.

[d] Twenty-five keV ^4He implanted in 15 μm thick foils of Ag and Cu.

[e] The experimental Doppler pattern together with τ_m = 420 fs is used to deduce the stopping power of Si in Mg, see text.

[f] Target of 200 μg/cm² TiT on thick Mg.

COINCIDENT HIGH-VELOCITY DSA LIFETIME MEASUREMENTS

Table 2 gives results for mean lives of low-lying levels in ^{28,29,30}Si obtained by bombardment of ^{2}H, ^{3}H and ^{4}He targets with a ^{28}Si beam. Concurrent investigations of stopping powers are discussed below.

The effective charge concept relates the electronic stopping power of an ion with a certain velocity in a given material to the stopping power of other ions with the same velocity in that material. Several authors have given formulae for such a scaling. Most recent is that proposed by Ziegler [2], who investigated experimental data for 127 ion-medium combinations, with ions ranging from ^{12}C to ^{238}U, energies from 200 keV/u to 22 MeV/u and media from Be to Au, both gaseous and solid. The heavy-ion electronic stopping powers generated from the proton stopping powers of Andersen and Ziegler [3] by means of Ziegler's scaling formula are reported [2] to have an accuracy of about 5 %. These scaled proton stopping powers are denoted as S_e^{SCAP}.

Figure 7 shows a comparison between S_e^{SCAP} and experimental data of Forster et al.[4] for F, Mg, Al, S and Cl ions slowed down in Ti, Fe, Ni, Cu, Ag and Au. The ratio of S_e^F (the experimental electronic stopping power from Forster et al.) and S_e^{SCAP} is plotted as a function of v/v_0 for the 30 ion-medium combinations.

For $v/v_0 > 8$ (equivalent to 1.6 MeV/u) the ratio differs less than 5 % from unity, so that at higher velocities the description of the slowing-down process by S_e^{SCAP} is quite adequate. For lower velocities, however, the difference is seen to be as large as 20 %.

It is also apparent from fig. 7 that for a given medium the ratio S_e^F/S_e^{SCAP} is quite similar for the different ions, as the remaining spread could be explained e.g. by the experimental error of about 5 % in S_e^F. Or phrased differently, the scaling from F to Cl is described correctly.

A simple explanation for the up to 20 % deviations from unity for the ratio S_e^F/S_e^{SCAP} could be the incorrectness of the used proton stopping powers, as in the calculation of S_e^{SCAP} the proton stopping power for a given medium is common to all ions slowing down in that medium. Inspection

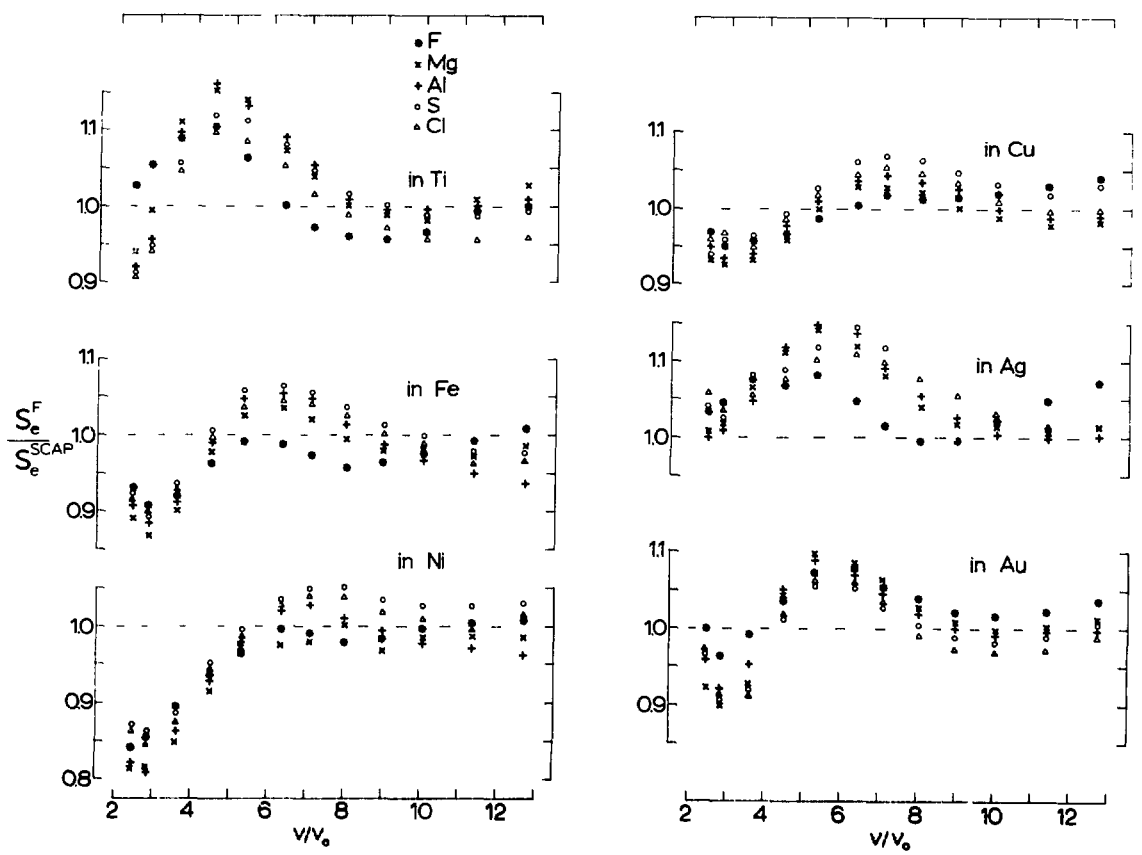

Fig. 7. A comparison between experimental electronic stopping powers of Forster et al. (S_e^F) and scaled proton values (S_e^{SCAP}) for ions of F, Mg, Al, S and Cl slowing down in Ti, Fe, Ni, Cu, Ag and Au. The ratio S_e^F/S_e^{SCAP} is plotted as a function of v/v_0 for the ion-medium combinations.

of the proton stopping data for the media of interest in the compilation of Andersen and Ziegler [3] makes clear that it is possible that their adopted proton stopping data could indeed be incorrect to such an extent.

The inadequacies observed in fig. 7 thus are as yet not necessarily to be blamed on the functional form of the scaling formula [2] or, more seriously, on the effective charge concept itself.

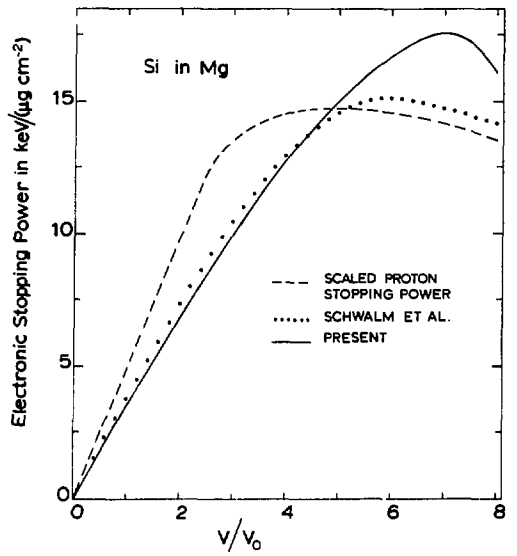

Fig. 8. The three electronic stopping powers for Si in Mg as discussed in the text.

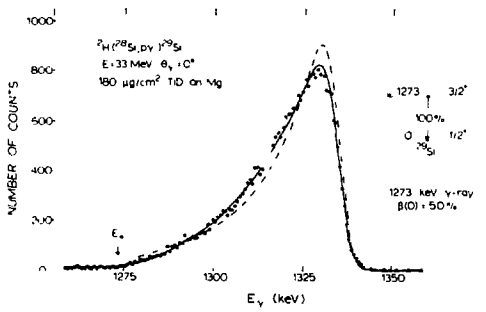

Fig. 9. The γ-ray Doppler pattern of the ^{29}Si(1.27 → 0 MeV transition for Mg as slowing-down material. The position of the stopped peak is given by E_0. The dashed line is the best result obtained for the stopping power S^{SCAP}. The drawn line corresponds to τ_m = 420 fs and the present stopping power S_{29}.

For the interpretation of Doppler patterns observed for excited Si ions slowing down in magnesium it is necessary to know the stopping of Si in Mg. Since direct experimental data are lacking, S_e^{SCAP}(Si → Mg) was calculated as outlined above.

The result is shown as the dashed line in fig. 8. Use of this S_e^{SCAP} stopping power in the analysis of the Doppler pattern measured for the 1.27 MeV, first excited state of ^{29}Si gave very poor results. The mean-life search yielded no value at all with an acceptable fit. The lowest χ^2 obtained was 5.3, corresponding to the dashed fit shown in fig. 9. This result implies that S_e^{SCAP}(^{29}Si → Mg) is certainly incorrect.

The dotted curve in fig. 8 represents the electronic stopping power of Si in Mg as given by Schwalm et al.[5]. Use of this stopping power improved the fit to the data of fig. 9 appreciably (lowest χ^2 = 2.2) but it was still not satisfactory.

The drawn line in fig. 8 is the stopping power obtained directly from the experimental Doppler pattern with the mean life kept fixed at τ_m = 420 fs. The latter mean life is obtained from separate experiments, in which Doppler patterns measured with Cu and Au backings are analysed with experimental stopping powers [4].

The stopping power for Si in Mg obtained in this way is denoted as S_{29}. It has an accuracy of about 5 % since it is basically the accuracy of the stopping powers for Si in Cu and Au. The accuracy of $S_{Schwalm}$ is also given as about 5 %. The error in S^{SCAP} is difficult to assess, as noted above.

The drawn line in the Doppler pattern of fig. 9 (with χ^2 = 1.5) corresponds to S_{29} and τ_m = 420 fs.

As a further test of S_{29} we have measured three additional Doppler patterns emitted by excited Si ions slowing down in Mg. The three states investigated are ^{28}Si (1.78 MeV, τ_m = 688 ± 26 fs), ^{29}Si (2.03 MeV, τ_m = 445 ± 14 fs) and ^{30}Si (2.24 MeV, τ_m = 363 ± 20 fs). The mean lives, which vary by almost a factor of two, are again obtained from separate experiments, in which Doppler patterns are analysed with experimental stopping powers [4].

The Doppler patterns measured with Mg are analysed with the three stopping powers S_{29}, $S_{Schwalm}$ and S^{SCAP}, discussed above, and the results are shown in fig. 10. The a priori known mean lives are indicated by the vertical arrows.

The result for ^{29}Si(1.27 MeV) is not surprising

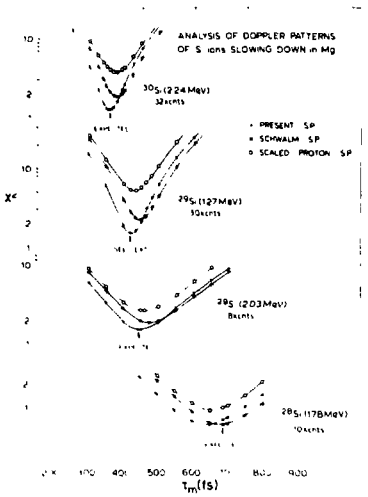

Fig. 10. Verification of the present stopping power S_{29}. The γ-ray Doppler patterns measured with Mg backing for ^{30}Si(2.24 MeV), ^{29}Si(1.27 MeV), ^{29}Si(2.03 MeV) and ^{28}Si(1.78 MeV) are analysed with the three stopping powers S_{29}, $S_{Schwalm}$ and S^{SCAP}. The figure shows for each of the four states the variation of χ^2 as a function of the mean life. The à priori known mean lives (see text) are indicated by the vertical arrows. The total number of coincidence counts in each pattern is also given.

since S_{29} was optimized for this level. For ^{30}Si(2.24 MeV) and ^{29}Si(2.03 MeV) the curves for S_{29} are lowest and dip at the expected values of τ_m. They thus corroborate S_{29}. The measurement for ^{28}Si(1.78 MeV) makes practically no distinction between S_{29} and $S_{Schwalm}$.

The χ^2 curves corresponding to S^{SCAP} are the worst for all four patterns. Nevertheless the lifetimes, deduced by means of S^{SCAP}, would have almost the correct value. In the analysis of a Doppler pattern it is thus possible to have a wrong stopping power, a bad fit but, nevertheless, a correct result. Inspection of fig. 8 shows that here this effect accidentally is due to the starting velocity of the Si recoils of $v(0)/v_0 \approx 7$. An experiment with a starting velocity of $v(0)/v_0 \approx 3$ would have yielded, independently of the lifetime, 35 % shorter lifetimes with S^{SCAP} than with S_{29}.

1) H.J.M. Aarts et al., to be published in Nucl. Instr.
2) J.F. Ziegler, Applied Phys. Lett. 31 (1977) 544.
3) H.H. Andersen and J.F. Ziegler, Hydrogen stopping powers and ranges in all elements (Pergamon Press New York, 1977).
4) J.S. Forster et al., Nucl. Instr. 136 (1976) 349.
5) D. Schwalm, E.K. Warburton and J.W. Olness, Nucl. Phys. A293 (1977) 425.

P.J. van Baal, A. Becker, A.J.H. Donné, O.A. van Herwaarden, A. Holthuizen, R. Kalish, G. van Middelkoop and A.J. Rutten

In the past year the transient magnetic field has been investigated for light ions in ferromagnetic Gd in continuation of measurements reported previously. Attention has also been paid to a comparison of the transient fields for ^{28}Si in various ferromagnetic materials to check whether or not the field strengths scale with the density of polarized electrons in the host. Finally, g-factors of short-lived excited states of ^{31}P have been measured. For this purpose the accurately calibrated transient field in Fe has been used.

THE FIELD IN Gd

Measurements of the transient field strength for light nuclei in Gd, kept at a temperature of 77 K, were intended to investigate possible atomic-shell effects in the atomic-number dependence of the field in Gd. Such effects were clearly found for Fe as a host (see Annual Report 1977). A qualitative interpretation of these measurements in Fe based on molecular orbital promotion in adiabatic atomic collisions led to the expectation that the Z-dependence of the field in Gd would have a discontinuity between Z = 10 and 12. Initial measurements (see Annual Report 1978) led to the conclusion that if such an effect would exist in Gd it is certainly much smaller than that in Fe.

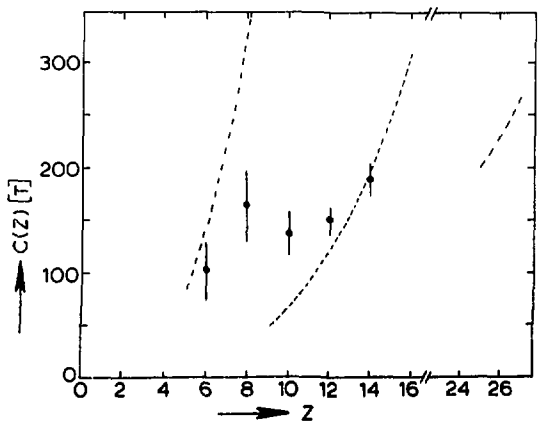

Fig. 1. The normalized transient field strength C(Z) as a function of ion atomic number in magnetized Gd at 77 K. The dashed curves represent the corresponding field strength in magnetized Fe.

In order to further clarify the situation, an experiment was performed at Z = 6. The $^{12}C(\alpha,\alpha')^{12}C$ reaction was used to excite the 2^+ state at 4.43 MeV (τ = 0.06 ps). In addition, previous measurements at Z = 12 and 14 were repeated in order to check reproducibility and to improve the accuracy. The ^{12}C experiment was done at an initial recoil velocity of $v_i \approx 4\ v_0$, whereas the ^{24}Mg and ^{28}Si experiments (confirming previous results) were performed at $v_i \approx 7v_0$ and $2v_0$, respectively. The resulting field strengths C(Z), normalized to a velocity $v = v_0$ by using the known proportionality of the field strength with velocity [1], are given in fig. 1. The C(Z) values are given for a polarized electron density equal to that of Fe. In order to facilitate a comparison with the transient field strength in Fe, the empirical C(Z) function for Fe is also given (dashed curves).

It is obvious that unlike the Z-dependence in Fe, the field strengths in Gd show a smooth dependence on the ion atomic number. The following comments may be made.

(i) The normalized field strengths for Z = 12 and 14 (Mg and Si) in Gd equal those found for Fe, which indicates a proportionality with the polarized electron density of the host as was found earlier for heavier ions [2].

(ii) For Z = 10 the field strength in Gd is significantly (more than three standard deviations) higher than that in Fe.

(iii) The fields are weaker in Gd than in Fe for $Z \leq 8$.

From this comparison of the present data with the data for Fe it seems that indeed between Z = 12 and 10 there is an increase in field strength which may extend to Z = 8. If there is such an effect at all it is certainly much less outspoken than in Fe. One might even say that the data points do not contradict a *linear* Z-dependence. Therefore one cannot draw a clear conclusion from these measurements. It may be not so surprising afterall that the Z-dependence for Gd is rather smooth since the coupling diagrams for light ions with Gd atoms involve many more molecular orbitals than those for the same ions with Fe atoms, thereby washing out shell effects.

OTHER FERROMAGNETIC HOSTS

From the above comparison of the dependence on ion atomic number for transient magnetic fields in Fe and Gd it seems well established that for $Z \geq 12$ the field strength scales with the density of polarized electrons in the ferromagnetic host (and not e.g. with the number of polarized electrons per host atom, i.e. 2.2 for Fe and 7.1 for Gd). It was therefore thought worthwhile to perform measurements for ^{28}Si at $v_i = 2v_0$ in Co and Ni in addition to those already carried out in Fe and Gd. For this purpose the first-excited 2_1^+ state of ^{28}Si was produced in the (α,α') reaction at the strong well-known resonance [3] at $E_\alpha = 7.50$ MeV.

To ensure that the ferromagnetic Co and Ni foils, with a typical thickness of 2-3 μm, were magnetized close to saturation (more than 90 %) during the experiments the absolute magnetization of such foils was first determined as a function of magnetizing field strength in a magnetometer. In addition the magneto-optical Kerr effect was used to check the surface magnetization [4]. The absolute magnetization found at the external strength applied in the transient field experiments was then used to convert the data to those for 100 % magnetized foils. The same procedure was followed for the Fe and Gd host measurements.

The results of these measurements for $^{28}Si(2_1^+)$ in Fe, Co, Ni and Gd hosts are given in fig. 2. In this figure the quantity $gC(Z)/n(\mu_B)$ is plotted versus $n(\mu_B)$, where g, C(Z) and $n(\mu_B)$ are the g-factor of $^{28}Si(2_1^+)$, the transient field strength at $v = v_0$ and the density of polarized electrons in the host (in n^{-3}), respectively. Clearly the data for Ni, Fe and Gd support the rule that the transient magnetic field scales with $n(\mu_B)$. The Co point, however, deviates significantly from the average value of the other three (by almost four standard deviations). Expressed differently, the normalized goodness-of-fit parameter for all points with the assumption of scaling with $n(\mu_B)$ is 4.3. The significant deviation for Co is at present not understood.

g-FACTOR MEASUREMENTS

The well-calibrated transient magnetic field for Z = 10 - 16 [refs. [1,5]] was used to measure the g-factors of the first two excited states of ^{31}P at 1.27 MeV ($J^\pi = 3/2^+$, $\tau_m = 0.75$ ps) and 2.23 MeV ($J^\pi = 5/2^+$, $\tau_m = 0.36$ ps). These states were populated with the $^{28}Si(\alpha,p)^{31}P$ reaction at $E_\alpha \approx 8.0$ MeV. Gamma-rays were detected in coincidence with protons at 180° to the beam direction. The optimum bombarding energies (giving a maximum in the reaction yield) were slightly different (50 keV) such that actually two measurements were performed. Since also the p-γ angular correlations differ for the two states, the γ-ray detection angles were set differently for these levels to take full advantage of the sensitivity to the small integral precession angles encountered.

The measured time-integral precession angles were found to be $\Delta\theta = 0.50 \pm 0.14$ and 1.97 ± 0.27 mrad corresponding to g-factors of $g = +0.17 \pm 0.05$ and $+0.95 \pm 0.14$ for the first and second excited state, respectively.

Shell-model wave functions obtained with matrix elements from Chung and Wildenthal [6] in an sd-shell configuration space truncated to at most four holes in the $d_{5/2}$ orbit and total seniority ≤ 5 yield g-factors for the first and second excited state of $g = +0.05$ and $+0.91$, respectively, which is in good agreement with the experimental results.

1) J.L. Eberhardt, R.E. Horstman, P.C. Zalm, H.A. Doubt and G. van Middelkoop, Hyperfine Interactions 3 (1977) 195.
2) J.M. Brennan, N. Benczer-Koller, M. Hass and H.T. King, Hyperfine Interactions 4 (1978) 268.
3) J.L. Eberhardt, R.E. Horstman, H.A. Doubt and G. van Middelkoop, Nucl. Phys. A244 (1975) 1.
4) P.C. Zalm, J. van der Laan and G. van Middelkoop, Nucl. Instr. 161 (1979) 265.
5) P.C. Zalm, A. Holthuizen, J.A.G. De Raedt and G. van Middelkoop, Hyperfine Interactions 5 (1978) 347.
6) G. van Middelkoop, Proceedings of the Fourth EPS Gen. Conf. (1979) 438.

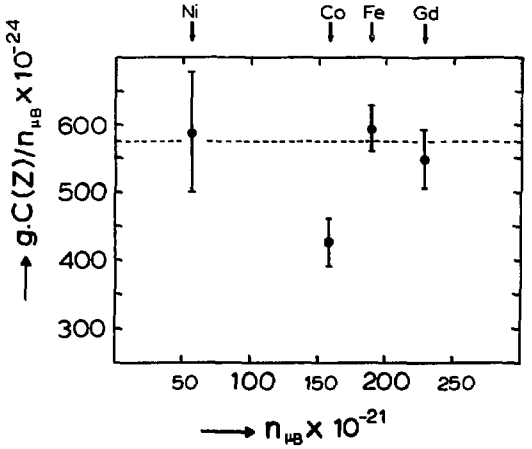

Fig. 2. The quantity $g.C(Z)/n(\mu_B)$ representing the transient field strength normalized to the polarized electron density $n(\mu_B)$ of the ferromagnetic host versus $n(\mu_B)$ for ^{28}Si ions recoiling into the host at a velocity of $v_i = 2v_0$.

1.3. Plunger experiments

A. Becker, C.P.M. van Engelen, A. Holthuizen, J. Kroon, G. van Middelkoop and A.J. Rutten

This chapter is a report on two different subjects which have in common that they involve recoil-distance measurements with plunger systems. The first subject is classical, it deals with a time-dependent deorientation g-factor and a lifetime measurement, partly reported on previously. The second subject deals with an attempt to measure nuclear spin deorientation in a free ion that has passed through a thin magnetized Fe foil. In this case part of the ions are expected to be polarized which should lead to a spin precession superimposed on a random deorientation.

g-FACTOR AND MEAN LIFE OF $^{20}O(2_1^+)$

The g-factor and the mean lifetime of the first-excited 2^+ state at 1.67 MeV have been determined with the recoil-into-vacuum deorientation and recoil-distance methods. For this purpose the $^3H(^{16}O,p)$ reaction at 24.5 MeV was used on a stretched ^3H-Ti-Ni target followed by a Ni stopper at variable distance. Gamma-rays were detected in coincidence with protons at 0^o to the beam axis at angles of 45^o and 90^o in large NaI(Tl) scintillation counters and in a 25 % Ge(Li) detector at 0^o (see Annual Report 1978).

The final analysis of the deorientation data (see fig. 1) in which populations of ionic ground state and isomeric excited-state electron configurations of one and two electron ions were taken into account yields a value of the g-factor of $|g| = 0.352 \pm 0.015$. The error includes uncertainties in the populations of the electron configurations, the zero distance of the target-stopper combination and the mean lifetime of the state. From the analysis it was found that 70 % of the single-electron ions are in their ground state and that 30 % of the two-electron ions are in an excited state. The mean life of the 2_1^+ state from this fit was found to be 10.3 ± 0.8 ps.

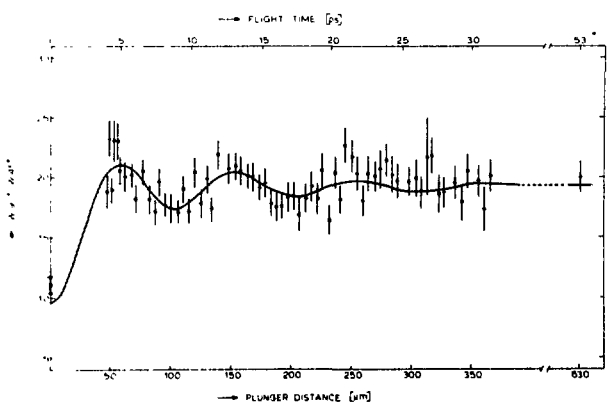

Fig. 1. The anisotropy $W(90^o)/W(45^o)$ of the p-γ angular correlation as a function of plunger distance together with a computer fit to the data.

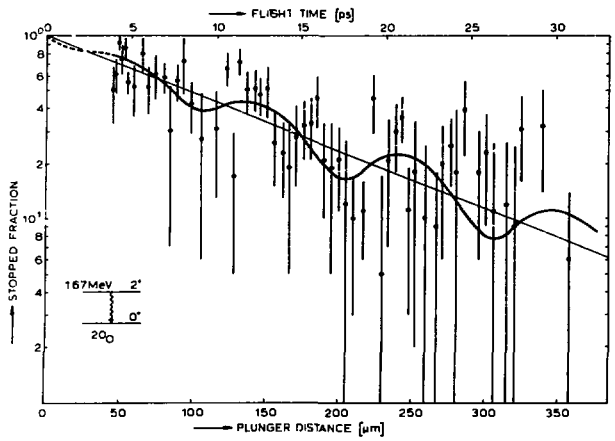

Fig. 2. The "stopped fraction" of γ-rays detected at 0^o to the beam direction in coincidence with protons at 0^o as a function of plunger distance. The fit to the data is a superposition of the time-dependent deorientation effect and an exponential decay; see text.

A more precise value for the lifetime was obtained from the spectra simultaneously measured with the Ge(Li) detector at 0^o to the beam direction. The ratio of the γ-ray intensity measured in the non-Doppler shifted line to the total photopeak intensity is given in fig. 2. These data were fitted with the time-differential deorientation obtained from the g-factor measurement superimposed on an experimental decay curve. In this fit the zero-distance of the plunger determined from the analysis of the NaI spectra was used such that the only

parameter in the fit was the mean life τ_m. This fit yields $\tau_m = 10.7 \pm 0.4$ ps. The weighted average of the determined mean lives therefore is $\tau_m = 10.6 \pm 0.4$ ps.

The presently measured value for the g-factor $g = -0.352 \pm 0.215$ [where the sign stems from ref. [1]] is in good agreement with the previously known [2] value of $g = -0.39 \pm 0.04$ but is much more precise. A shell-model calculation by Arima et al.[3] yields a value of $g = -0.15$, whereas a more sophisticated calculation [4] with modified Kuo-Brown matrix elements leads to a value of $g = -0.34$. Clearly the latter is in good agreement with the present experimental value.

For the mean life two values were previously known. A plunger measurement [2] yielded $\tau_m = 14.2 \pm 0.8$ ps and a DSA measurement [5] $\tau_m = 9.8 \pm 0.7$ ps. The present value of $\tau_m = 10.6 \pm 0.4$ ps clearly rules out the previous plunger measurement and is in good agreement with the DSA value.

FREE-ION PRECESSION?

One of the crucial tests of the atomic picture of the transient magnetic field phenomenon would be to observe *directly* a polarization of the recoiling ion after passage *through* magnetized iron. This polarization can be observed if the nucleus of the ion is excited to a state with a lifetime of the order of 10 ps. In that case one may observe, superimposed on the time-dependent deorientation, a net *"precession"* of the nuclear spin in a recoil-into-vacuum plunger experiment by means of γ-ray detection in an array of counters.

In order that this time-dependent effect is measurable with a plunger one needs ion velocities of the order of a few percent of the speed of light. For light ions ($Z < 9$) recoiling at such velocities in magnetized Fe we know that an appreciable fraction of the ions has a single *polarized* 1s electron, which is responsible for the observed strong transient magnetic field. If we use a thin magnetized foil (2 μm) through which the ions recoil into vacuum at $v/c \approx 5$ % we may expect that, if the Fe surface is sufficiently clean, still a fraction of some 20 % of the ions is polarized in vacuum. A good candidate for such an experiment is ^{16}O excited in its 3_1^- state with a mean lifetime of $\tau_m = 27$ ps.

In the past year the theory which describes the nuclear spin deorientation in ions with *polarized* electrons has been developed. This involves the description of the time-dependent perturbation of the angular distribution of γ-rays emitted in the decay of the aligned nuclear state due to the hyperfine interaction between the nuclear dipole moment and the dipole moment of the (polarized) 1s electron. The formulation of this theory is a straightforward extension of the processes describing ordinary deorientation [6].

This calculation has been applied to the specific case of excited ^{16}O recoiling through a thin magnetized Fe foil. The 3_1^- state (with $g = +0.55 \pm 0.04$) is produced and aligned with the $^1H(^{19}F,\alpha)$ reaction at $E(^{19}F) = 48.1$ MeV with the outgoing α-particles detected at 0° to the ^{19}F beam direction. The recoil velocity after passage through the ^1H-Ti target on a 2 μm thick Fe foil amounts to $v = (6.6 \pm 0.3)v_0$, in which $v_0 = c/137$.

The perturbation of the α-γ angular correlation consists of three parts.

(i) A small transient-field effect *during* the passage of the excited ^{16}O ions through the magnetized Fe foil.

(ii) An ordinary deorientation effect in the free ^{16}O *after* the passage through the Fe foil due to the fraction of ions which is *not* polarized.

(iii) A "precession" of the ion about its total angular momentum $\vec{F} = \vec{I} + \vec{J}$ due to the polarized ion fraction.

The effects (i) and (iii) induce changes in γ-ray counting rates of opposite sign in detectors placed in the horizontal plane at angles symmetric about the (horizontal) beam direction. The effects are largest at angles where the logarithmic derivative of the α-γ angular correlation has a maximum. The transient-field precession angle is, after the ions have left the foil, fixed and amounts to $\Delta\theta \approx 8$ mrad. The "deorientation precession" continues as time develops and causes largest counting rate effects at these angles after certain time intervals (for the present case 1, 3, 5, 7 ... ps). Moreover the effects *change sign* at each consecutive point of time (i.e. it is positive at 1 and 5 ps after the ions leave the foil and negative at 3 and 7 ps). By using pairs of γ-ray detectors one can form the usual double ratios of counting rates. The effect (ii) yields counting-rate changes that are identical in detectors placed symmetric about the beam. In addition these effects are close to zero at angles sensitive to the precession effects.

The calculations yield a transient field and a "deorientation precession" double ratio of 3 % and ± 20 %, respectively. Hence the searched effect is clearly detectable.

For the experiment a special plunger set-up has been constructed which allows one to stretch and magnetize the Fe target foil, with stoppers at prefixed distances of 14, 43, 72 and 101 μm,

corresponding to the above-mentioned time intervals. The first experiment failed, however, due to imperfect stoppers which allowed too much spread in the recoil distance.

If it turns out that a sizeable effect exists it is not only a test of the atomic model for the transient magnetic field but it would also enable one to produce (partly) polarized beams of non-zero spin nuclei. For that purpose transmission of a beam through a thin magnetized Fe foil followed at a certain distance by a non-magnetic depolarizer foil would polarize transversely part of the beam.

1) J. Gerber, M.B. Goldberg and K.H. Speidel, Phys. Lett. 60B (1976) 338.
2) Z. Berant, C. Broude, G. Engler, M. Hass, R. Levy and B. Richter, Nucl. Phys. A243 (1975) 519.
3) A. Arima, Nucl. Phys. A108 (1968) 94.
4) W. Chung, Ph. D. thesis (Michigan State University, 1976).
5) J.A.J. Hermans, G.A.P. Engelbertink, L.P. Ekström, H.H. Eggenhuisen and M.A. van Driel, Nucl. Phys. A284 (1977) 307.
6) H. Frauenfelder and R.M. Steffen, in Alpha-, beta- and γ-ray Spectroscopy, ed. K. Siegbahn, vol. 2 (North-Holland, Amsterdam, 1965).

1.4. Radiocarbon dating with a tandem accelerator

K. van der Borg, R. Kamermans, A.M. Hoogenboom and A. Vermeer

In the past two years it has been shown [1,2] that highly sensitive mass spectrometry can be performed with nuclear accelerators. Especially a group in Rochester (N.Y.) [1] showed that a tandem is eminently suited for the detection of trace isotopes. The detection efficiency of this method is higher by orders of magnitude than that of conventional methods, so that for ^{14}C dating purposes the sample size and measuring time can become much smaller. In addition it is expected that the time span of the usual method (based on measuring the ^{14}C radioactivity) can be extended by at least 20 000 years.

Since even in a recent sample the ratio of $^{14}C/^{12}C$ is only $\approx 10^{-12}$, stringest requirements have to be met for the rejection of ions of the wrong mass and/or charge. This can be done by the combination of different selection principles like magnetic and electrostatic rigidity and by using a gasfilled heavy-ion counter [see ref. 1]. Suppression of the main contaminent ^{14}N can be obtained easily with a tandem by making use of the fact that $^{14}N^-$ ions are too shortlived to become accelerated.

In the fall of this year a start has been made with the design of a 12° electrostatic analyser and with the construction of the Rochester heavy-ion counters I and II [ref. 1 and 3]. Experiments on the sputter ion source and on the stabilization of the tandem by means of the generating voltmeter are described in ch. 6.

1) K.H. Purser, A.E. Litherland and H.E. Gove, Nucl. Instr. 162 (1979) 637.
2) E.J. Stephenson, T.S. Mast and R.A. Muller, Nucl. Instr. 158 (1979) 571.
3) D. Elmore and R. Ferraro, Rochester Annual Report (1978) p. 174.
D. Shapira et al., Nucl. Instr. 129 (1975) 123.

2. RESEARCH WITH THE 4 MV ACCELERATOR

2.1. Capture reactions

M. Adachi, F.M. Bloemen, A. Buijs, C. Dommisse, P.J.M. Hoppenbrouwers, C. van der Leun, S. van der Meij, G.J.L. Nooren, A.P. Riethoff, J.J.A. Smit

A Compton-suppression spectrometer and three conventional Ge(Li) detectors of 80, 95 and 100 cm^3 have been used in the experiments listed below.

$^{22}Ne(p,\gamma)^{23}Na$

Thin targets have been prepared by bombarding tantalum backings with 2-3 keV ^{22}Ne ions. These targets withstand 1 MeV proton beams of up to 200 μA for many hours.

$^{36}S(p,\gamma)^{37}Cl$

A yield curve has been measured in the range E_p = 0.5 - 2.0 MeV. The installation of a sliding shorting rod made it possible to study the low-energy range. This resulted in the observation of twelve new resonances in the range E_p = 0.5 - 0.8 MeV (see fig. 1).

The energies and strengths of the 180 observed resonances have been determined. Resonances in the $^{27}Al(p,\gamma)^{28}Si$ and $^{34}S(p,\gamma)^{35}Cl$ reactions served as energy calibration standards; $^{32}S(p,\gamma)^{33}Cl$ and $^{34}S(p,\gamma)^{35}Cl$ resonances as strengths standards. From the complete list, which is available upon request, we quote our values for the well-known $J^\pi = 7/2^-$, T = 5/2 isobaric analogue resonance: E_p = 1886.6 ± 0.4 keV and S = 32 ± 3 eV, which should be compared to the literature values E_p = 1 888.6 ± 0.4 keV and S = 24 ± 3 eV, respectively.

Inhomogeneities in the target often cause problems in strength measurements. Over an energy range of 100 keV, yield variations of up to 20 % have been observed due to the small changes in place and size of the beam spot which inevitably occur during standard resonance-curve measurements. These variations have been reduced to an acceptable level by placing a narrow diaphragm (diam. 1 mm) in front of the target.

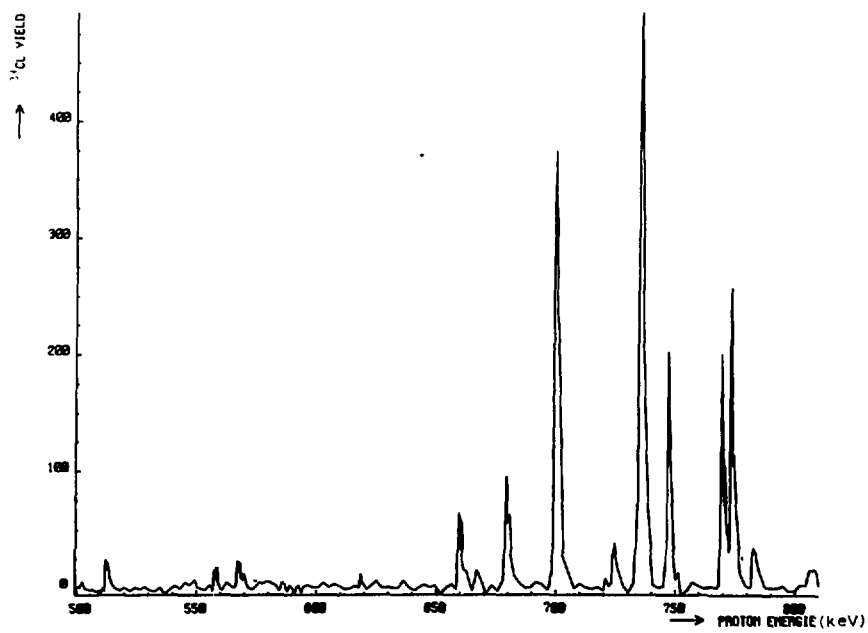

Fig. 1. The $^{36}S(p,\gamma)^{37}Cl$ yield curve in the range E_p = 500 - 800 keV.

At the resonances in the range E_p = 0.5 - 1.2 and 1.8 - 2.0 MeV, with the exception of a few very weak ones, γ-ray spectra have been measured at $\theta = 55^o$ and 90^o. The analysis of these spectra established the decay schemes and thus makes it possible to select resonances for angular distribution measurements.

The first angular distributions have been measured at E_p = 824 and 899 keV. For this purpose Ag_2S targets have been made on Cu backings. These targets withstand considerably higher beam currents (up to 100 μA) than those on the usual Ta backings. The first spins deduced from these data are $J^\pi = 1/2^+$ and $5/2^+$ for the E_p = 824 and 899 keV resonances, respectively.

$^{54}Fe(p,\gamma)^{55}Co$

The decay has been studied of nine resonances in the range E_p = 0.7 - 1.5 MeV. This also yields the decay scheme of 20 bound states of ^{55}Co. The excitation energies of the lowest ^{55}Co levels, all based on the 1978 "gold-standard" [3] are listed in table 1.

TABLE 1. Excitation energies of ^{55}Co levels

E_x(eV)	E_x(eV)
2 165 940 ± 25	2 939 590 ± 50
2 565 795 ± 25	3 303 590 ± 150
2 659 510 ± 50	3 324 500 ± 200
2 918 540 ± 160	3 563 150 ± 40

Angular distributions have been measured at E_p = 1225, 1328 and 1476 keV. The analysis is in progress. The first results are $J^\pi = 7/2^-$ and 3/2 for $^{55}Co^*$ = 2.92 and 3.56 MeV, respectively.

1) P.M. Endt and C. van der Leun, Nucl. Phys. A310 (1978) 1.

2) P.M. Endt, Atomic Data and Nuclear Data Tables 23 (1979) 3.

3) R.G. Helmer, P. Van Assche and C. van der Leun, Atomic Data and Nuclear Data Tables (to be published).

2.2. Resonance absorption and fluorescence

E.L. Bakkum, R.J. Elsenaar, J. Hop, H. Lancman, C. van der Leun, J.H. Nokkert and F. Zijderhand

Monoenergetic γ-rays of variable energy, provided by (p,γ) reactions on light nuclei, have been used in nuclear photoexcitation experiments of both unbound and bound nuclear levels [1].

ABSORPTION

$^{11}B(\gamma,\gamma)^{11}B$

Gamma-rays from the E_p = 1417 keV $^{23}Na(p,\gamma)^{24}Mg$ resonance have been used in resonance absorption experiments on the 8.92 MeV level of ^{11}B. The classical [2] method of analysis applied to these data, leads to level widths for ^{11}B(8.92 MeV) that are strongly dependent on the length of the ^{11}B absorber.

Special attention has therefore been given to the interaction of the γ-rays with the absorbing atoms in the crystal lattice. Lamb [2] treated the crystal as a Debye continuum. The absorption line then has the same shape as for a gas, but one has to use an effective temperature T_{eff} instead of the temperature T of the crystal. The T_{eff} corresponds to the average energy per vibrational degree of freedom in the lattice. The line shape is a Voigt profile.

The velocity distribution of the vibrating crystal atoms, and consequently the line shape and T_{eff}, depend on the type of binding in the crystal. Three simple velocity distributions have been taken as example to calculate the influence on T_{eff} and $\Gamma_{\gamma 0}$:

(i) a classical harmonic oscillator, with an average energy kT per degree of freedom, resulting in a rather broad double-peaked line shape;

(ii) a Maxwellian distribution of the maximum oscillator velocity, resulting in a sharply peaked line shape;

(iii) a block-shaped velocity distribution that results in a broad line shape.

Model (ii) leads to a rather consistent set of $\Gamma_{\gamma 0}$ values for the different absorber lengths. Lambs theory, however, still leads to the best results if one uses the purely empirical temperature of $\frac{1}{4} T_{eff}$ (see fig. 1).

Further experiments with different absorber materials are planned to study these effects in more detail.

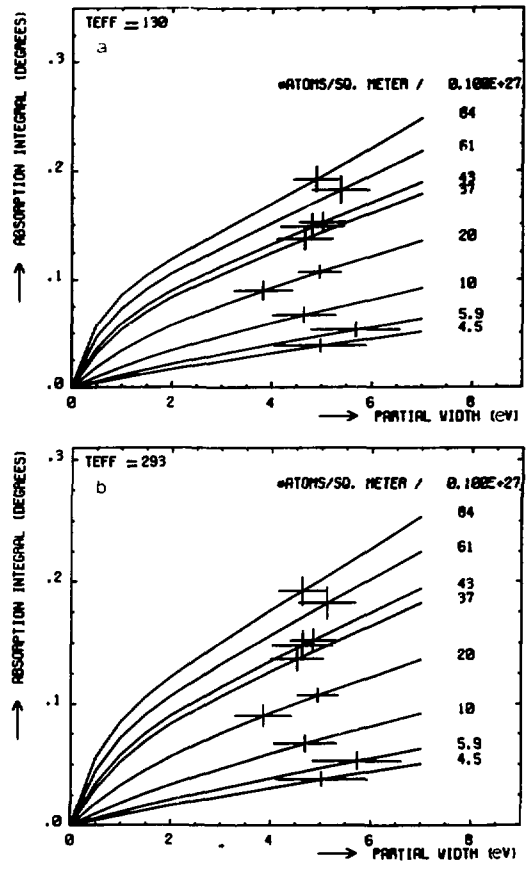

Fig. 1. Width of the 8.92 MeV level of ^{11}B deduced from γ-ray absorption measurements with different absorber lengths,

a) with Lamb's theory, but with a temperature of $T_{eff}/4$, and

b) for a Maxwellian distribution of the maximum oscillator velocity.

$^{28}Si(\gamma,\gamma)^{28}Si$

The 1958 resonant absorption measurement of Smith and Endt [3] on the 12.33 MeV level of ^{28}Si (the E_p = 774 keV $^{27}Al(p,\gamma)^{28}Si$ resonance) has been repeated.

The present experiment has been performed with Ge(Li) detectors, such that it was feasible to separate the 10.55 MeV r → 1.78 MeV from the 12.33 MeV r → 0 transition. For three different lengths of the Si absorber, the transmission has been measured at 30 angles around the resonance angle (see fig. 2). With the recent value for the resonance strength of S = 5.9 ± 0.5 eV [4], the measured absorption integrals lead to the value Γ_{γ_0}(12.33) = 6.6 ± 0.8 eV, in good agreement with the values from (e, e') experiments: Γ_{γ_0} = 5.9 ± 0.3 eV [5] and 7.3 ± 1.9 eV [6]. Comparison with the 1958 resonant absorption value of Γ_{γ_0} = 5.2 ± 0.5 eV [3] is not valid, since the latter is based on a superseded value for the resonance strength.

If one uses in the analysis $\frac{1}{4}$ T_{eff} instead of the classical T_{eff}, it leads to a more consistent set of Γ_{γ_0} values. The effect, however, is less pronounced than in the case of ^{11}B, where the absorber has a considerably higher Debye temperature than the present Si absorber.

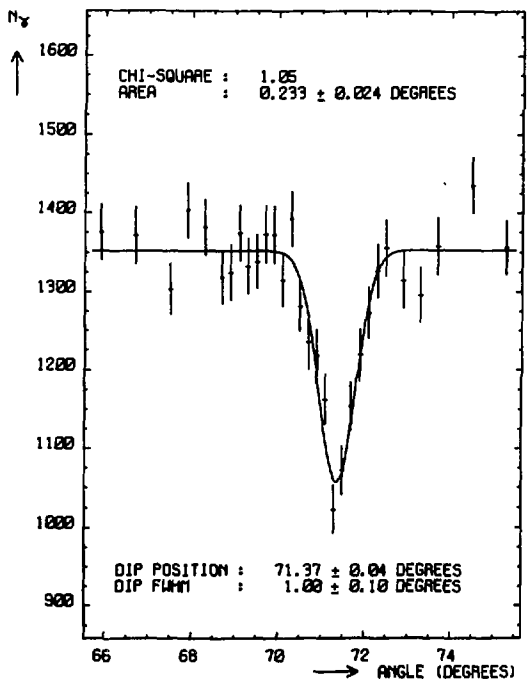

Fig. 2. Absorption of 12.33 MeV gamma rays from the $^{27}Al(p,\gamma)^{28}Si$ reaction in a 94 mm long Si absorber.

FLUORESCENCE

$^{23}Na(\gamma,\gamma)^{23}Na$

The E_x = 9147 ± 5 keV level of ^{23}Na [6] has been excited by γ-rays from the E_p = 1748 keV $^{13}C(p,\gamma)^{14}N$ resonance. The observed resonance angle, α_r = 109.08° ± 0.14°, combined with recent values [7,8] for the reaction Q-value (Q = 7550.63 ± 0.02 keV) and the resonance energy (E_p = 1747.6 ± 0.9 keV), leads to $E_x(^{23}Na)$ = 9153.3 ± 0.8 keV.

Although the signal-to-background ratio in the resonant fluorescence experiment is considerably better than in a resonant absorption experiment, the background is still too high to use this case for further study of the resonant fluorescence technique.

$^{205}Pb(\gamma,\gamma)^{208}Pb$

The 7.06 MeV (J = 1) level of ^{208}Pb has previously been excited in a resonant absorption experiment [9] by γ-rays from the E_p = 2542 keV $^{34}S(p,\gamma)^{35}Cl$ resonance. The same level has presently been excited in a resonant fluorescence experiment by γ-rays from the same source. It turns out that for the determination of the resonant angle, the fluorescence experiment has twice the sensitivity of the absorption experiment. This is essentially due to the low background in the resonant fluorescence experiment.

For the determination of the level width, however, an additional self-absorption experiment has to be performed to obtain a result that is in first approximation independent from the geometry of the set-up and from the absolute detector efficiency.

1) A.P.M. van 't Westende, H. Lancman and C. van der Leun, Nucl. Instr. 151 (1978) 205.
2) W.E. Lamb, Phys. Rev. 55 (1939) 19.
3) P.B. Smith and P.M. Endt, Phys. Rev. 110 (1958) 397.
4) P.M. Endt, Atomic Data and Nucl. Data Tables 23 (1979) 3.
5) R. Schneider et al., Nucl. Phys. A323 (1979) 13.
6) L.W. Fagg et al., Phys. Rev. 187 (1969) 1378.
7) A.H. Wapstra and K. Bos, Atomic Data and Nucl. Data Tables 19 (1977) 175.
8) F. Ajzenberg-Selove, Nucl. Phys. A268 (1976) 1.
9) R.J. Sparks, H. Lancman and C. van der Leun, Nucl. Phys. A259 (1976) 13.

2.3. Precision calibration of gamma-ray energies

C. Alderliesten, P.F.A. Alkemade, S. Bazna-Lucardi, C. van der Leun, J.A. van Nie and P. de Wit

A set of γ-ray energies in the range E_γ = 0.06 - 3.50 MeV, all with uncertainties of at most 10 ppm, is available for the energy calibration of γ-ray spectra. It is a consistent set in the sense that all these energies are based on the value [1] of E_γ = 411 804.4 ± 1.1 eV for the γ-ray from the decay of ^{198}Au. In order to extend this energy range, the energy of the 6.13 MeV transition in ^{16}O has been measured in terms of this gold-standard.

Since the 6.13 MeV level itself decays exclusively to the ^{16}O ground state, the cascade-crossover technique could not be applied directly. The E_p = 319 and 391 keV resonances in the reaction ^{25}Mg(p,γ)^{26}Al, which both decay by γ-rays of about 6.2 MeV and also by cascading low-energy γ-rays, were therefore used as intermediate steps.

The error due to the Doppler shift of the (p,γ) lines could be reduced to an acceptable level by precise alignment of the set-up and by measuring at angles θ = +90° and -90° with respect to the proton beam. Calibration of the non-broadened 6.13 MeV line from a ^{13}C(α,n)^{16}O source against the Doppler broadened peaks from reaction γ-rays, made it necessary to calculate centroids instead of using the standard peak-fitting procedures. This increases the statistical error, which is the largest single error (≈ 40 eV) in the final result E_γ = 6 129 270 ± 50 eV. The latter value is the average of a series of measurements with different spectrometers and several different settings of the electronics.

In the calibration of the 6.13 MeV γ-rays on the 6.2 MeV lines of ^{26}Al one uses, in addition to the precise peak positions, the local dispersion at this high energy. At the present level of precision it is not allowed to use for this purpose the 511 keV distances between full-energy, single- and double-escape peaks. This problem has been tackled by separate precision measurements of the excitation energies of the lower bound states of ^{26}Al. These data make it possible to calculate the energy differences for the E_γ = 5 - 6 MeV primary transitions from ^{25}Mg(p,γ)^{26}Al resonances very precisely, and thus provide precise values for the local dispersion at high γ-ray energies. The necessity of this somewhat cumbersome procedure is clearly demonstrated by the value that for one detector has been found for the distance between single- and double-escape peaks: 510 630 ± 90 eV. This value seems to be independent from E_γ, but might very well be detector dependent.

The energies of the ^{26}Al levels listed in table 1 are a byproduct from this dispersion calibration.

A more detailed account of these experiments is given in refs. [3,4].

Another extension of the set of γ-ray calibration lines is possible by precision measurements of the energies of the γ-rays in the decay of ^{66}Ga. The spectrum of this source, which decays with a half-life of about 10 h, contains useful γ-rays up to E_γ = 4.81 MeV.

Sources have been produced with the tandem accelerator in the reaction ^{63}Cu(α,n)^{66}Ga at E_α = 18 MeV. Spectra are measured simultaneously with a conventional Ge(Li) detector and with a Compton-suppression spectrometer. The data reduction is in progress. It will lead to energies with a precision that meets the quality standard of the IUPAP task-group for γ-ray energy calibration standards, i.e. better than 10 ppm.

TABLE 1. Energies of some bound states of ^{26}Al (E_x in eV)

Present work	Literature [2]
228 305 ± 13	228 440 ± 150
416 852 ± 3	416 800 ± 300
1 057 739 ± 12	1 057 700 ± 500
1 759 034 ± 8	1 759 000 ± 500
1 850 620 ± 70	1 850 300 ± 600
2 365 150 ± 18	2 365 000 ± 400
2 545 367 ± 17	2 545 200 ± 500
2 660 920 ± 50	2 660 800 ± 400
2 740 030 ± 30	2 739 200 ± 700
2 913 400 ± 50	2 913 000 ± 500
3 159 889 ± 13	3 159 600 ± 700
3 724 860 ± 70	3 723 200 ±1200

1) E.G. Kessler et al., Phys. Rev. Lett. 40 (1978) 171.
2) P.M. Endt and C. van der Leun, Nucl. Phys. A310 (1978) 1.
3) C. van der Leun, R.G. Helmer and P. Van Assche, Proceedings AMCO 6, (Plenum Press, 1979).
4) P.F.A. Alkemade et al., Nucl. Instr. (to be published).

3. THERMAL NEUTRON CAPTURE

J.R. Balder, Ginevra Delfini, P.M. Endt, J.F.A.G. Ruyl, A. Tielens and R. Vennink

THE $^{23}Na(n,\gamma)^{24}Na$ REACTION

Gamma-gamma angular correlations have been measured in a 500 h run with the Ge-Ge set-up described in the 1977 Annual Report. These data have been analysed in conjunction with the results of previous measurements [1] of the circular polarization of γ-rays produced upon capture of polarized neutrons. This work has provided the γ-ray mixing ratios of 17 transitions and the channel spin mixing parameter α of 7 primary transitions (see table 1).

The α-values found are all quite small or, in other words, thermal capture predominantly proceeds through the 1^+ channel. If the α-values are weighted with the primary intensities one obtains $\langle\alpha\rangle_{av} = 0.04 \pm 0.01$. This is in agreement with earlier work which had shown that the main contribution to the thermal capture cross section derives from the strong 1^+ resonance at $E_n = 2.85$ keV; the capture γ-ray spectra at thermal energy and at 2.85 keV are identical. No transitions are observed to 3^- or 4^+ states in ^{24}Na which, if the capture proceeds via the 1^+ channel, would have M2 and M3 character, respectively; transitions to 3^+ states (with E2 character) are quite weak.

TABLE 1. Results of $^{23}Na(n,\gamma)^{24}Na$ γ-γ angular correlation measurements (unpolarized neutron capture) combined with γ-ray circular polarization measurements (polarized neutron capture) [a]

$E_{xi} \rightarrow E_{xf}$ (MeV)	$J_i^\pi \rightarrow J_f^\pi$	δ	α [b]
1.344 → 0.56	$3 \rightarrow 2^+$	+0.02 ± 0.04	
2.51 → 0.56	$3^+ \rightarrow 2^+$	−0.04 ± 0.14	
2.98 → 0.47	$2^+ \rightarrow 1^+$	+0.7 ± 0.6	
→ 0.56	$\rightarrow 2^+$	−0.09 ± 0.05	
→ 1.341	$\rightarrow 2$	−0.11 ± 0.06	
→ ..344	$\rightarrow 3$	+0.20 ± 0.14	
3.37 → 0.56	$2^- \rightarrow 2^+$	−0.20 ± 0.06	
→ 1.344	$\rightarrow 3$	+0.1 ± 0.2	
3.59 → 0.56	$1^+ \rightarrow 2^+$	+0.19 ± 0.07	
4.44 → 0.56	$2^- \rightarrow 2^+$	−0.06 ± 0.05	
→ 1.344	$\rightarrow 3$	0.02 ± 0.09	
4.75 → 0.56	$2^- \rightarrow 2^+$	+0.13 ± 0.18	
C → 0.56	$1^+ \rightarrow 2^+$	−0.04 ± 0.02 [c]	0.010 ± 0.008 [c]
→ 1.341	$\rightarrow 2$	+0.04 ± 0.06 [d]	0.11 ± 0.06 [d]
→ 2.98	$\rightarrow 2^+$	+0.11 ± 0.03	$0.139^{+0.006}_{-0.019}$
→ 3.37	$\rightarrow 2^-$	+0.02 ± 0.05	0.08 ± 0.03
→ 3.59	$\rightarrow 1^+$	$-1.0^{+0.6}_{-1.7}$	0.17 ± 0.13
→ 4.44	$\rightarrow 2^-$	+0.02 ± 0.06	0.001 ± 0.004
→ 4.75	$\rightarrow 2^-$	$-0.5^{+0.7}_{-4.4}$	0.0 ± 0.3

a) Data from ref. [1].

b) Defined as $\alpha = I(2^+)/\{I(1^+) + I(2^+)\}$.

c) A second solution is $\delta = +2.14 \pm 0.13$, $\alpha = 0.07 \pm 0.02$.

d) A second solution is $\delta = -3.5 \pm 0.7$, $\alpha = 0.002 \pm 0.013$.

THE $^{45}Sc(n,\gamma)^{46}Sc$ REACTION

A considerable amount of previous work has been performed on this reaction, in particular through the capture of polarized neutrons on a polarized target at thermal energy [2], and on the capture of unpolarized neutrons at low-energy resonances [2,3]. The spectrum from unpolarized neutrons at thermal energy, however, is not known in great detail. Yet the detailed knowledge of the singles spectrum is essential for the interpretation of the data previously taken.

Consequently, a 14 day measurement was performed of the singles spectrum (E_γ > 2 MeV) with the Petten pair spectrometer. The target consisted of 6 g Sc_2O_3. In addition, the low-energy part of the spectrum (E_γ < 2 MeV) was measured with a "bare" Ge detector. The analysis of these spectra is in progress.

THE $^{56,58}Fe(n,\gamma)^{57,59}Fe$ REACTIONS

The measurement of the singles spectra resulting from these reactions (reported in the 1978 Annual Report) has formed a chapter in the thesis of R. Vennink. A paper on the subject has been submitted to Nuclear Physics.

1) J. Kopecky, F. Stecher-Rasmussen and K. Abrahams,
Petten Report RCN-175 (1972).

2) H.I. Liou, R.E. Chrien, J. Kopecky and J.A. Konter,
Nucl. Phys. to be published.

3) M.J. Kenny, B.J. Allen and R.L. Macklin,
Austral. J. Phys. 30 (1977) 605.

4. THEORY

4.1. Shell-model calculations on fp-shell nuclei

R.C.H. Broers, Ginevra Delfini, P.W.M. Glaudemans, B.C. Metsch, A.G.M. van Hees, R.B.M. Mooy, G.A. Timmer, G.N.A. van Veen, R. Vennink and D. Zwarts

A continuation of the theoretical investigation of medium-heavy nuclei turns out to be quite rewarding because (i) the nuclei not too far from the doubly-magic $^{56}_{28}Ni_{28}$ core can be treated quite well with the shell model and (ii) these nuclei exhibit some interesting collective properties. This makes a further study feasible of the relation between microscopic and collective properties.

So far we have studied several isotopes of $_{24}Cr$, $_{25}Mn$, $_{26}Fe$, $_{27}Co$, $_{28}Ni$ and $_{29}Cu$. In most cases the configuration space is restricted to fp-shell orbits where the number of holes in the $f_{7/2}$ orbit is one larger than in the simplest shell-model space. For example we take into account four $f_{7/2}$ holes in ^{53}Fe and one $f_{7/2}$ hole in Ni or Cu isotopes. A brief account of some of the results obtained is presented below.

EFFECTIVE INTERACTIONS

All calculations have been performed with at least two quite different interactions. We have investigated in detail a slightly modified Kuo-Brown interaction (KB) and the Surface Delta Interaction (SDI). Both interactions have good and bad features. The KB interaction is superior when the $f_{7/2}$ hole structure dominates the properties, whereas SDI gives much better results when particles in the $p_{3/2}$, $f_{5/2}$ and $p_{1/2}$ orbits are important. It is therefore not surprising that for the Co isotopes no clear preference exists for either KB or SDI. This is illustrated in fig. 1 with the decay scheme of ^{57}Co. In this calculation the $^{54-58}Co$ isotopes are treated in a model space including up to two $f_{7/2}$ holes. Although for Ni isotopes SDI works considerably better than KB, since they are dominated by their particle structure, this does not hold, however, for all observables. Examples are the magnetic dipole moments of the lowest $J^\pi = 5/2^-$ states. The SDI wave functions yield values which are very close to the Schmidt value but deviate strongly from experiment, whereas KB nicely reproduces the experimental values. The difference between KB and SDI is found to depend on the values of only five out of 155 two-body matrix elements. When one replaces these five SDI matrix elements of the type $\langle f_{7/2} f_{5/2} | V | f_{5/2} f_{5/2} \rangle_{JT}$ by those of KB one finds for SDI dipole moments which are in good agreement with experiment.

A search has been started for an effective interaction combining the good features of both SDI and KB for the nuclei investigated in the present model space.

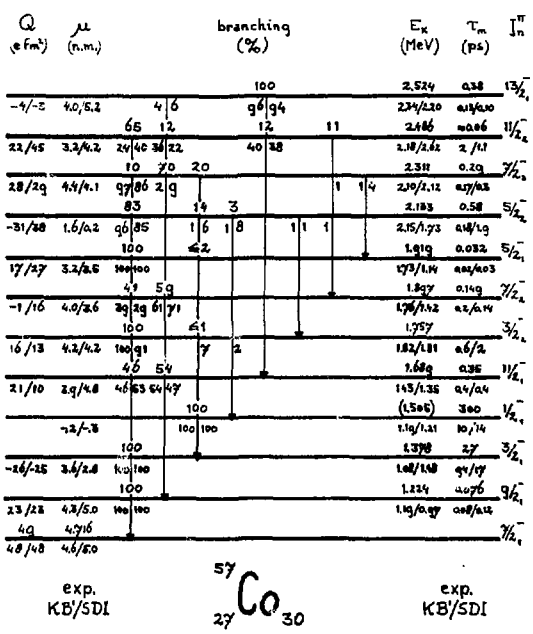

Fig. 1. Comparison between calculated and experimental decay scheme of ^{57}Co. For each of the properties shown, i.e. quadrupole moment, magnetic moment, branching ratio, lifetime and excitation energy, the number just above the line represents the experimental value (taken from R.L. Auble, Nucl. Data Sheets 20 (1977) 327). The numbers below each line give the KB/SDI theoretical values.

COLLECTIVE PROPERTIES AND HIGH-SPIN STATES

There are indications that ^{53}Fe and ^{56}Fe exhibit interesting collective properties. Both nuclei have been investigated with KB and SDI two-body matrix elements. One finds that for ^{53}Fe the KB interaction gives rise to a very simple collective interpretation of the properties of some yrast and yrast-plus-one states. Not only the excitation energies of these states but also their electromagnetic properties nicely follow the behaviour expected for a pure K = 1/2 band, see figs. 2 and 3. These collective properties do not show up in the SDI wave functions for ^{53}Fe.

The excitation energies of the lowest ten states of each J in ^{56}Fe calculated with KB are plotted in fig. 4. With SDI nearly identical results are obtained. Of the many states shown in fig. 4 some are of a remarkable nature. From a calculation of the E2/M1 transition rates it follows that all yrast states and many of the yrast-plus-one states can be classified in groups. The members within each group are connected by relatively strong transitions, see fig. 5 for the SDI result. The KB result is quite similar except for the important difference that the K = 0 ground-state band for KB stops at $J^{\pi} = 8^{+}$. It would be very interesting to test these model predictions experimentally.

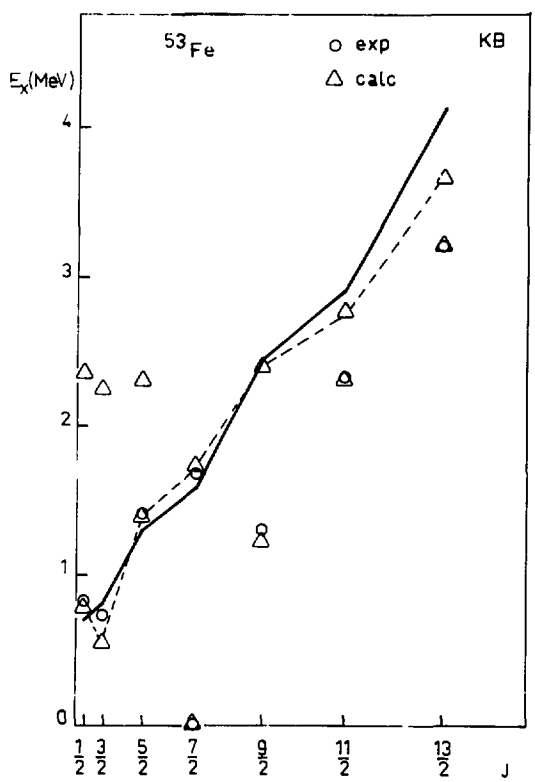

Fig. 2. Calculated (KB) and experimental excitation energies of ^{53}Fe versus J(J+1). The triangles denote the shell-model values calculated with KB. The dashed line connects the shell-model results and the solid line represents the collective model values for a pure K = 1/2 band.

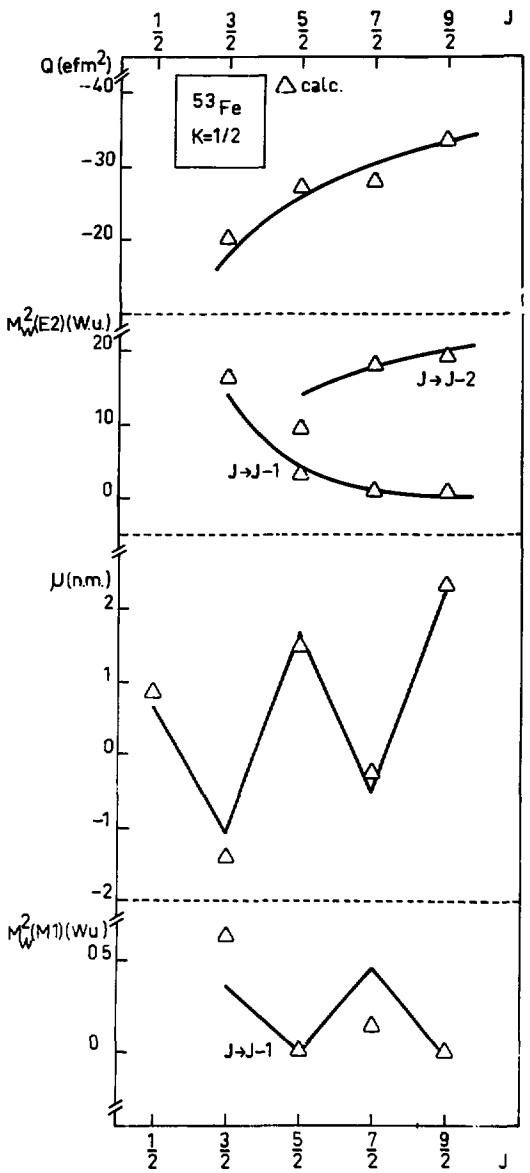

Fig. 3. Comparison of electromagnetic properties calculated with the shell model for the KB interaction (triangles) and the collective model (solid line) for a pure K = 1/2 band.

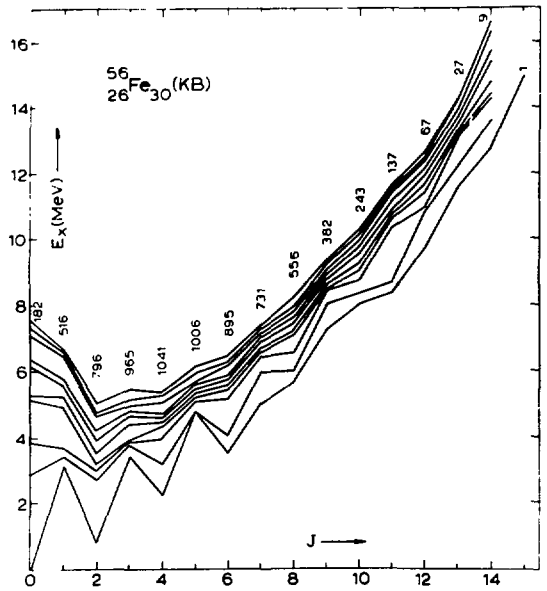

Fig. 4. Excitation energies of the lowest ten states with positive parity of each J obtained with the KB interaction for ^{56}Fe. The vertically placed numbers represent the total number of states for each J in the present model space.

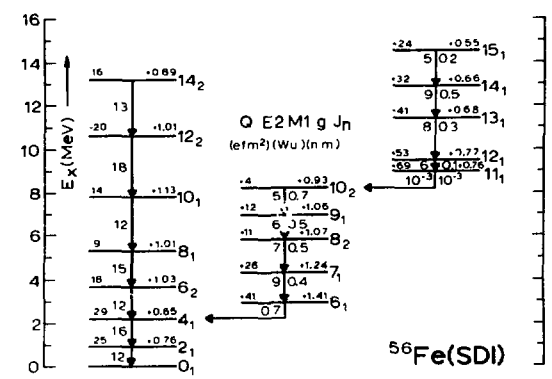

Fig. 5. Electromagnetic properties of selected states in ^{56}Fe obtained with SDI. The quadrupole and dipole moments as well as E2 and M1 transition strengths are displayed as is indicated on top of the second group of states.

TRANSITIONS OF HIGH MULTIPOLARITY

Very little is known about the behaviour of high-multipolarity transitions in the fp-shell. A well-known problem is presented by the strengths of the E6, M5 and E4 transitions occurring in the decay of the $19/2^-$ state in ^{53}Fe. It follows that $f_{7/2}^{-4}(p_{3/2}f_{5/2}p_{1/2})^1$ admixtures strongly affect these transitions as is shown for KB and SDI in fig. 6.

Work on the distribution of M8 strengths in ^{58}Ni, ^{54}Fe and ^{56}Fe is in progress. It seems that the experimentally observed phenomena can be reproduced qualitatively in a model space in which one particle is excited out of the $f_{7/2}$ orbit into the $g_{9/2}$ orbit, while recouplings between active particles in the $p_{3/2}$, $f_{5/2}$ and $p_{1/2}$ orbits are taken into account.

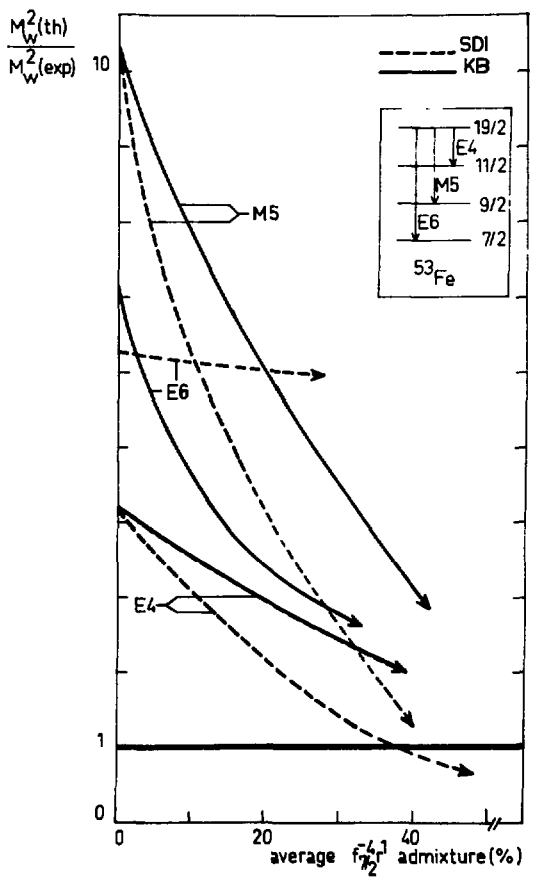

Fig. 6. Strengths of the E6, M5 and E4 transitions for the decay of the $19/2^-$ state in ^{53}Fe calculated with KB and SDI as a function of the intensity of four-hole admixtures. Bare-nucleon charges and g-factors are used.

TRUNCATION PROCEDURES

For an extension of the present calculations to higher masses and for a study of the effects of more $f_{7/2}$ holes in the A $\approx$ 56 nuclei a reliable truncation of the configuration space is necessary.

A new method has been investigated in which first all diagonal Hamiltonian matrix elements are calculated and arranged according to increasing excitation energy. Secondly only those off-diagonal matrix elements have been calculated that connect the lower-lying pure states with all other pure states in the interaction matrix. The remaining very large group of off-diagonal matrix elements is assumed to be zero. One thus calculates only a narrow band of matrix elements in the Hamiltonian matrix. This method has been applied to ^{56}Fe and ^{57}Fe and its results have been compared with an exact calculation. So far the method seems to work better than previously investigated truncation methods.

4.2. Statistical methods

P.J. Brussaard and J.J.M. Verbaarschot

As the inclusion of the full fp shell in a model calculation leads to configuration spaces that are far too large to handle, it is desirable to possess a well-founded algorithm for a truncation procedure. A statistical approach to the description of eigenvalue spectra and eigenvector components could possibly lead to such a procedure that does not require the diagonalization of extremely large energy matrices.

Investigation of the distribution of the amplitudes of the eigenvectors in the full sd shell of $J^\pi = 1^+$ states of ^{22}Na (dimension 243) and $J^\pi = 1/2^+$ states of ^{25}Mg (dimension 1434) has shown that the secular variation of the amplitudes can be described in very good approximation in terms of only the centroids and widths (i) of the distribution of the diagonal matrix elements of the Hamiltonian and (ii) of a particular distribution of the amplitudes. The fluctuations of the amplitudes can be described in terms of a Porter-Thomas distribution. The distribution of the eigenvector amplitudes is non-Gaussion, however.

4.3. Atomic shell-model calculation

B.C. Metsch and G.A. Timmer

The available nuclear shell-model programs have been applied to the atomic spectra of Ir and Os. The atomic spectra of positive parity could be reproduced, but those of negative parity still show appreciable deviations.

5. REVIEW ACTIVITIES

P.M. Endt and C. van der Leun

A-CHAIN REVIEWS

The literature scan on A = 21-44 nuclei is continued. The 7th edition of this review is planned to appear in 1983.

Our recent extensive use of Nuclear Data Sheets (see below) has led to the preparation of a note presenting our views on the principles of A-chain reviewing. This note should serve as a basis for a discussion on this subject at the April 1980 meeting of the IAEA Nuclear Data Section.

GAMMA-RAY STRENGTHS

A review of γ-ray strengths in A = 6-44 nuclei has appeared in 1979 [1].

For some transitions there is a marked A-dependence; for instance, the strengths of E1 and M1 transitions decrease with A. It seemed interesting to investigate whether these trends continue for A > 44.

For this purpose a review has been prepared [2] of γ-ray strengths in the A = 45-90 region; it contains 1200 transitions (against 2400 transitions for A = 6-44). The main body of input data could be taken from Nuclear Data Sheets, but a considerable number of additional papers had also to be scanned for more recent data. The A = 45-90 region shows some notable differences with A = 6-44. First, it does not supply any isospin retarded transitions. Second, the number of suitable transitions from unbound states is quite small. And finally, the influence of electron conversion (and the corresponding difference in photon branchings and total branchings) has to be well accounted for.

In fig. 1 strength histograms are shown for M1,

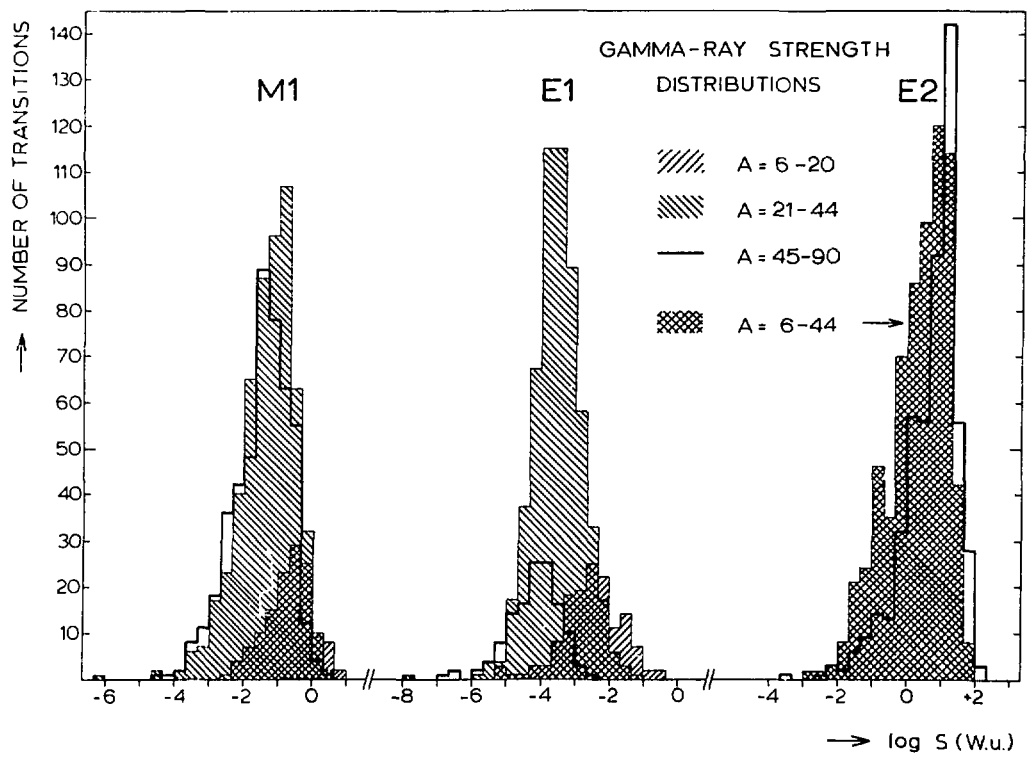

Fig. 1. Strength histogram of M1, E1 and E2 γ-ray transitions for the A = 6-20, 21-44 and 45-90 regions. The logarithmic abscissa scale indicates the strength in Weisskopf units. For E2, the curves for the lower and middle A-regions differ so little that they are represented by a single histogram. The figure clearly shows a large decrease of strength with A for E1, a small decrease for M1, and a small increase for E2.

E1 and E2 in very light nuclei (A = 6-20), light nuclei (A = 21-44) and medium-heavy nuclei (A = 45-90). One can conclude that the strength decrease with A for M1 and E1 continues into the A = 45-90 region, whereas E2 strengths increase (for the latter, the A = 6-20 and 21-44 regions show no observable difference). The strongest E2 transitions are found in the upper half of the A = 45-90 region. These findings are understandable, because one expects single-particle character to decrease and collective character to increase with A.

The data have been used to extract recommended upper limits for A = 45-90 γ-ray strengths. In table 1 they are compared to those for lighter nuclei. In addition to E1 and M1, also M2 strengths seem to decrease with A.

In fig. 2 the number of γ-ray transitions with known strength is plotted as a function of A. It shows that nuclear spectroscopy on medium-heavy nuclei (in particular A = 70-90) is still relatively "underdeveloped" as compared to that on lighter nuclei.

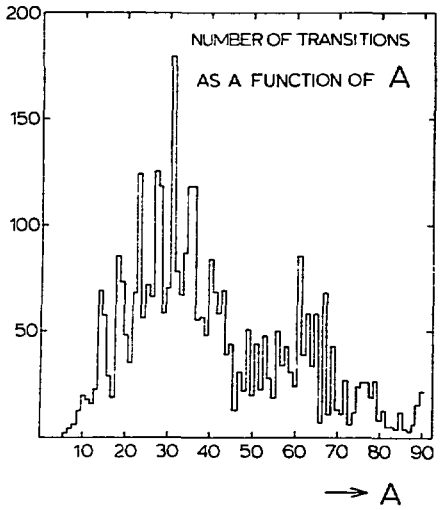

Fig. 2. The number of γ-ray transitions with known strength as a function of A.

TABLE 1. Recommended upper limits (RUL) in the A = 6-20, 21-44 and 45-90 regions

Character [a]	Number of Transitions			RUL (W.u.)		
	A = 6-20	21-44	45-90	A = 6-20	21-44	45-90
E0	8	13	4			
$E1_{IV}$	139	567	127	0.3	0.1	0.01
$E1_{IS}$	36	100		0.003	0.003	
$E2_{IS}$	112	562	515	100	100	300
$E2_{IV}$	11	10		10	10	
E3	16	37	45	100	100	100
E4	3	7	17	100	100	100
E5	1	1	3			
$M1_{IV}$	135	559	470	10	10	3
$M1_{IS}$	13	31		0.03	0.03	
$M2_{IV}$	8	37	15	3	3	1
$M2_{IS}$	4	4		0.1	0.1	
$M3_{IV}$		4	7	10	10	10
$M3_{IS}$		1				
M4			8			30
M5	1					

[a] With the indices IV and IS denoting isovector and isoscalar character, respectively.

TABLE 2

GAMMA-RAY CALIBRATION ENERGIES

Source	E_γ(eV)	Source	E_γ(eV)	Source	E_γ(eV)
^{182}Ta	67 750.0 ± 0.2	$^{108}Ag^m$	614 281 ± 4	^{182}Ta	1 231 016 ± 5
^{153}Gd	69 673.4 ± 0.2	$^{110}Ag^m$	620 360 ± 3	^{56}Co	1 238 287 ± 6
^{170}Tm	84 255.1 ± 0.3	^{124}Sb	645 855 ± 2	^{182}Ta	1 257 418 ± 5
^{182}Ta	84 680.8 ± 0.3	$^{110}Ag^m$	657 762 ± 2	^{182}Ta	1 273 730 ± 5
^{153}Gd	97 431.6 ± 0.3	^{137}Cs	661 660 ± 3	^{22}Na	1 274 542 ± 7
^{182}Ta	100 106.5 ± 0.3	^{198}Au	675 887.5 ± 1.9	^{182}Ta	1 289 156 ± 5
^{153}Gd	103 180.7 ± 0.3	$^{110}Ag^m$	677 623 ± 2	^{59}Fe	1 291 596 ± 7
^{182}Ta	113 672.3 ± 0.4	$^{110}Ag^m$	687 015 ± 3	^{124}Sb	1 325 512 ± 6
^{182}Ta	116 418.6 ± 0.7	^{144}Ce	696 510 ± 3	^{60}Co	1 332 502 ± 5
^{152}Eu	121 782.4 ± 0.4	^{94}Nb	702 645 ± 6	^{56}Co	1 360 206 ± 6
^{57}Co	122 061.4 ± 0.3	$^{110}Ag^m$	706 682 ± 3	^{124}Sb	1 368 164 ± 7
^{192}Ir	136 343.4 ± 0.5	^{124}Sb	713 781 ± 5	^{24}Na	1 368 633 ± 6
^{57}Co	136 474.3 ± 0.5	^{124}Sb	722 786 ± 4	^{182}Ta	1 373 836 ± 5
^{182}Ta	152 430.8 ± 0.5	$^{108}Ag^m$	722 929 ± 4	$^{110}Ag^m$	1 384 300 ± 4
^{182}Ta	156 387.4 ± 0.5	^{95}Zr	724 199 ± 5	^{182}Ta	1 387 402 ± 5
^{182}Ta	179 394.8 ± 0.5	$^{110}Ag^m$	744 277 ± 3	^{124}Sb	1 436 563 ± 7
^{182}Ta	198 353.0 ± 0.6	$^{110}Ag^m$	763 944 ± 3	$^{110}Ag^m$	1 475 788 ± 6
^{192}Ir	205 795.5 ± 0.5	^{124}Sb	790 712 ± 7	^{144}Ce	1 489 160 ± 5
^{182}Ta	222 109.9 ± 0.6	$^{110}Ag^m$	818 031 ± 4	$^{110}Ag^m$	1 505 040 ± 5
^{182}Ta	229 322.0 ± 0.9	^{54}Mn	834 843 ± 6	$^{110}Ag^m$	1 562 302 ± 5
^{228}Th	238 632 ± 2	^{56}Co	846 764 ± 6	^{228}Th	1 620 735 ± 10
^{152}Eu	244 698.9 ± 1.0	^{228}Th	860 564 ± 5	^{124}Sb	1 690 980 ± 6
^{182}Ta	264 075.5 ± 0.8	^{94}Nb	871 119 ± 4	^{207}Bi	1 770 237 ± 10
^{203}Hg	279 196.7 ± 1.2	^{192}Ir	884 542 ± 2	^{56}Co	1 771 350 ± 15
^{192}Ir	295 958.2 ± 0.8	$^{110}Ag^m$	884 685 ± 3	^{56}Co	1 810 722 ± 17
^{192}Ir	308 456.9 ± 0.8	^{46}Sc	889 277 ± 3	^{88}Y	1 836 063 ± 13
^{192}Ir	316 508.0 ± 0.8	^{228}Th	893 408 ± 5	^{56}Co	1 963 714 ± 12
^{51}Cr	320 084.2 ± 0.9	^{88}Y	898 042 ± 4	^{56}Co	2 015 179 ± 11
^{152}Eu	344 281.1 ± 1.9	$^{110}Ag^m$	937 493 ± 4	^{56}Co	2 034 759 ± 11
^{198}Au	411 804.4 ± 1.1	^{124}Sb	968 201 ± 4	^{124}Sb	2 090 942 ± 8
^{192}Ir	416 471.9 ± 1.2	^{56}Co	1 037 844 ± 4	^{56}Co	2 113 107 ± 12
$^{108}Ag^m$	433 936 ± 4	^{124}Sb	1 045 131 ± 4	^{144}Ce	2 185 662 ± 7
$^{110}Ag^m$	446 811 ± 3	^{207}Bi	1 063 662 ± 4	^{56}Co	2 212 921 ± 10
^{192}Ir	468 071.5 ± 1.2	^{198}Au	1 087 691 ± 3	^{56}Co	2 598 460 ± 10
^{7}Be	477 605 ± 3	^{59}Fe	1 099 251 ± 4	^{228}Th	2 614 533 ± 13
^{192}Ir	484 577.9 ± 1.3	^{65}Zn	1 115 546 ± 4	^{24}Na	2 754 030 ± 14
^{207}Bi	569 702 ± 2	^{46}Sc	1 120 545 ± 4	^{56}Co	3 009 596 ± 17
^{228}Th	583 191 ± 2	^{182}Ta	1 121 301 ± 5	^{56}Co	3 201 954 ± 14
^{192}Ir	588 585.1 ± 1.6	^{60}Co	1 173 238 ± 4	^{56}Co	3 253 417 ± 14
^{124}Sb	602 730 ± 3	^{56}Co	1 175 099 ± 8	^{56}Co	3 272 998 ± 14
^{192}Ir	604 414.6 ± 1.6	^{182}Ta	1 189 050 ± 5	^{56}Co	3 451 154 ± 13
^{192}Ir	612 465.7 ± 1.6	^{182}Ta	1 221 408 ± 5	"^{16}O"	6 129 270 ± 50

Recommended by a IUPAP task group. For details and references, see R.G. Helmer, P.H.M Van Assche and C. van der Leun, Atomic Data and Nuclear Data Tables (1980).

GAMMA-RAY ENERGIES

The IUPAP Commission on Atomic Masses and Fundamental Constants established a task-group for the production, recommendation and publication of a consistent set of energy calibration standards for use in γ-ray spectroscopy.

The first recommendation of the task-group [3,4] presents a consistent set of 126 γ-ray energies in the range E_γ = 60-6100 keV, all with uncertainties of at most 10 ppm (see table 2). All energies are based on the recent value of E_γ = 411 804.4 ± 1.1 eV for the γ-ray from the decay of ^{198}Au.

1) P.M. Endt,
Atomic Data and Nuclear Data Tables, 23 (1979) 3.

2) P.M. Endt,
accepted for publication in Atomic Data and Nuclear Data Tables.

3) C. van der Leun, R.G. Helmer and P. Van Assche, Proceedings AMC06; Plenum Press (1979).

4) R.G. Helmer, P. Van Assche and C. van der Leun, accepted for publication in Atomic Data and Nuclear Data Tables.

6. EXPERIMENTAL EQUIPMENT

A. Vermeer and collaborators (see p. 2)

THE TANDEM ACCELERATOR

The number of tandem running hours amounted to 4100 h for 1979, somewhat less than the average of 4800 h over the last ten years (see fig.1). The reason is the (temporary) lack of a leader for one of the two main groups using the machine.

A slit system has been installed in the beam line directly behind the source inflection magnet. Both the positions and the widths of the vertical and horizontal slit jaws can be adjusted by remote control, and they can be read on a digital display. The system not only improves the facility with which the beam can be aligned, but it also serves to decrease the accelerator load by removing unwanted beam components.

The power supply has come ready for the sputter source of the Aarhus type. This supply, installed in a high-voltage cage, produces the extraction and control voltages, and the magnet and arc currents. On a first test a ^{12}C beam has been accelerated, but some small improvements still have to be effected. It can be expected that the source can be taken into full use in early 1980.

Some research has been performed on the conductance for gas flow of the accelerating tube of an EN tandem [1]. Such a tube, made up of a large number of metal electrodes separated by pyrex insulating rings, constitutes a rather complicated vacuum system. In fig. 2 some measurements are shown, both on a straight tube and on an inclined field tube. It can be seen that at low pressure, in the molecular flow region, the conductance is independent of the pressure. The measured conductances are in excellent agreement with those calculated by means of a theoretical model.

THE 4 MV AND 1 MV ACCELERATORS

The 4 MV Van de Graaff made 2500 running hours in 1979.

Thanks to improvements of the extraction system of the hf ion source [2], this generator now delivers analysed proton beams exceeding 200 μA. To measure the current in the unanalysed beam a high-power Faraday cup was installed (see fig. 3). The beam is stopped in a Ta cup which can heat up to over 2000 °C. The radiation heat is collected by the water-cooled Cu housing. The cup can handle 6 kW.

In order to increase the beam current at voltages below 1 MV a HVEC shorting rod assembly has been installed which can shortcircuit part of the column. The improvement obtained for protons is shown in fig. 4. The voltage at which the current drops below 50 % of full beam has been decreased from 800 kV to 350 kV.

It has been tried to reduce the terminal ripple

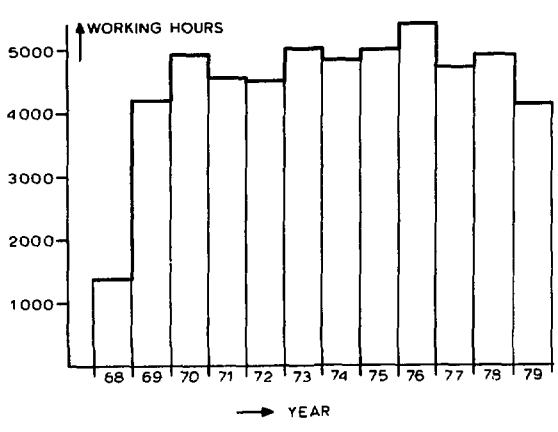

Fig. 1. Yearly working hours of the EN tandem since 1968.

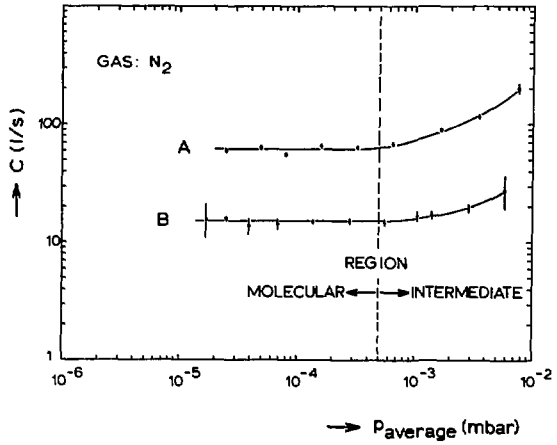

Fig. 2. Gas flow through EN accelerator tube as a function of pressure (average of those at the ends); A, straight tube, B, inclined field tube.

by adding to the power supply providing the upcharge current an alternating voltage with the belt frequency and adjustable phase. The result is encouraging, in particular if also harmonics of the belt frequency are added.

The 1 MV accelerator has been largely used for atomic physics experiments.

THE DATA HANDLING SYSTEM

The two PDP 11/40 computers have been replaced by PDP 11/34's, with which data collection has become faster and more reliable.

A fast ADC interface for analyser simulation has been installed for use with the 4 MV machine. It handles up to eight ADC's simultaneously with a data feed-through of 120 kHz.

ELECTRONICS

Some preliminary experiments have been performed to stabilize the tandem terminal voltage by means of the generating voltmeter. A stability of 2 kV for terminal voltages between 4 and 6 MV can be reached. The necessity for this stabilization system derives from the planned use of the tandem for ^{14}C dating, where expected currents are far too small for the usual stabilization system based on the currents on the jaws of the vertical slit behind the 90° deflection magnet.

Two high-quality pulsers have been developed for calibration of the analog electronics used in precision γ-ray energy measurements. The differential and integral non-linearities of the total analog chain can be measured down to 0.1 % and 0.002 %, respectively.

1) A. Vermeer and N.A. van Zwol, submitted to Nucl. Instr.

2) A. Vermeer and A.J. Veenenbos, Nucl. Instr. 163 (1979) 309.

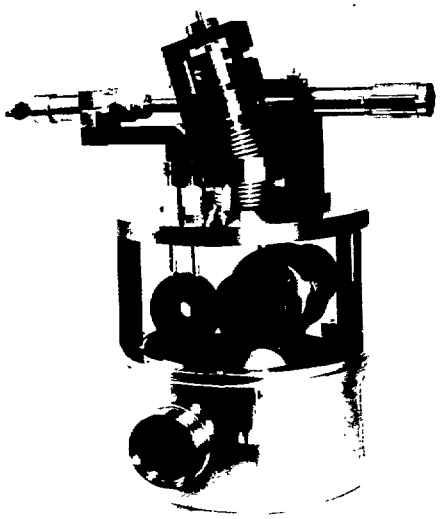

Fig. 3. High-power Faraday cup in use with 4 MV Van de Graaff.

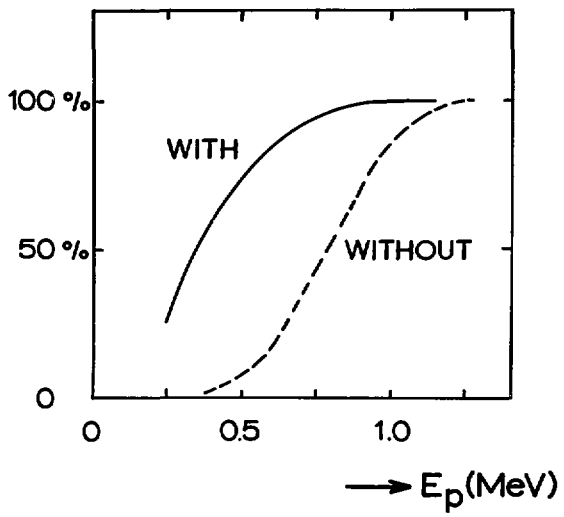

Fig. 4. Low-energy proton beam currents from 4 MV Van de Graaff with and without shorting rod (typical beam currents at 1.2 MV are 120-200 μA).

I.E.1: 3.A

Nuclear Physics **A321** (1979) 515–532; © *North-Holland Publishing Co., Amsterdam*

HIGH-SPIN YRAST LEVELS OF ^{38}Ar

H. J. M. AARTS, G. A. P. ENGELBERTINK, H. H. EGGENHUISEN † and L. P. EKSTRÖM ††

Fysisch Laboratorium, Rijksuniversiteit, Utrecht, The Netherlands

Received 27 October 1978

Abstract: High-spin states of ^{38}Ar have been studied with the ^{35}Cl(α, pγ)^{38}Ar reaction at E_α = 18 MeV and with the ^{24}Mg(^{16}O, 2pγ)^{38}Ar reaction at $E(^{16}O)$ = 38 and 45 MeV. The ^{38}Ar level scheme is obtained with the former reaction from a proton-γ coincidence measurement. Gamma-gamma coincidence, γ-ray angular distribution and linear polarization experiments have been performed with a Ge(Li)-Na(Tl) Compton suppression spectrometer and a three-crystal Ge(Li) Compton polarimeter. Unambiguous spin-parity assignments of $J^\pi = 7^-$, 7^+, 8^+, 7^-, 9^- and 11^- to the ^{38}Ar levels at E_x = 7.51, 8.08, 8.57, 8.97, 10.17 and 11.61 MeV, respectively, are obtained. The 8.57 MeV, 8^+ level has a mean life below 0.8 ps. Excitation energies, branching ratios, multipole mixing ratios and transition strengths are reported. The experimental results are compared with shell-model calculations.

E

NUCLEAR REACTIONS ^{35}Cl(α, pγ)^{38}Ar, E = 18 MeV; measured pγ-coin; ^{38}Ar deduced levels; ^{24}Mg(^{16}O, 2pγ)^{38}Ar, E = 38 and 45 MeV; measured $\sigma(E_\gamma, E)$, $\sigma(E, \theta)$, $\gamma\gamma$-coin, γ-ray lin. polarization, Doppler pattern; ^{38}Ar deduced levels, $T_{1/2}$, γ-branching, J, π, δ, transition strengths. Enriched targer, HP Ge, Compton suppression spectrometer, three-crystal Ge(Li) Compton polarimeter.

1. Introduction

Experiments with heavy-ion fusion-evaporation (HIFE) reactions, in which the basic properties of the HIFE process are exploited, have shown that these reactions are very suitable for detailed nuclear structure investigations of low-lying yrast states of light nuclei. High-spin levels in ^{38}Ar have been studied previously with the ^{27}Al(^{14}N, 2pnγ)^{38}Ar reaction [1]) and the ^{24}Mg(^{16}O, 2pγ)^{38}Ar reaction [2]), both at bombarding energies of about 40 MeV.

The ^{35}Cl(α, pγ)^{38}Ar reaction at E_α = 14 MeV has been used [3]) in an extensive investigation of ^{38}Ar levels up to 10 MeV excitation energy. From this work it became clear that in the HIFE studies mentioned above the measurement of γ-ray energies, intensities, (apparent) lifetimes and coincidence relations was not sufficient for the construction of the decay scheme in a unique way. Generally, arguments concerning the time order of γ-rays, which are based on intensity or

† Present address: Philips Research Laboratories, Eindhoven, The Netherlands.
†† Present address: Oliver Lodge Laboratory, Liverpool, Great Britain.

Transient magnetic fields acting on nuclei moving through ferromagnetic media

G van Middelkoop
Fysisch Laboratorium, Rijksuniversiteit, PO Box 80 000, 3508 TA Utrecht, The Netherlands

Abstract. The transient magnetic field experienced by nuclei moving in magnetised ferromagnetic media is discussed experimentally and theoretically with emphasis on light nuclei in iron and gadolinium. The merits of an atomic model are discussed and a couple of alternative interpretations are touched upon.

1. Introduction

The strong (kilotesla) transient magnetic field, experienced by nuclei *during* their slowing down in magnetised ferromagnetic media was discovered by Borchers *et al* (1966 and 1968). This field, which is unidirectional and aligned with the external field used for magnetising the host, is well suited for measuring magnetic moments of short-lived (picosecond) excited nuclear states. For this purpose one requires an adequate description of the transient field. Not only is it a tool in nuclear spectroscopy but also an interesting phenomenon itself.

A tentative qualitative explanation of this transient phenomenon has been given by Borchers *et al* (1968). They suggested 'that possibly the field arises from the net pick-up of polarised electrons from the iron as the recoil ion neutralises.' We will see later that this suggestion is close to the truth at least for light ions.

A more quantitative description has been presented by Lindhard and Winther (1971). They show that Coulomb scattering of (polarised) host electrons at the moving ion leads to an enhanced polarised electron density at the nucleus. The resulting field strength agrees to within a factor of two with the experimental values for ions with atomic number $Z_1 \geqslant 26$ and for low recoil velocities ($v < 3v_0$; $v_0 = c/137$). The calculated field strength is inversely proportional to the ion velocity for $v > v_0$ and essentially proportional to the atomic number of the moving ion.

The Lindhard and Winther theory, adjusted in one parameter to fit experimental values, had been used up to about 1975 for the analysis of spin precession measurements of magnetic moments; see e.g. Hubler *et al* (1972, 1974) and Eberhardt *et al* (1974).

It then became clear, due to experiments on light nuclei at relatively high recoil velocities, that the Lindhard–Winther theory is seriously inadequate. This has again led to studies of the transient field phenomenon itself. The experimental results and a microscopic, qualitative, interpretation form the main subject of the present paper.

1.E.3:
2.B

Nuclear Physics **A315** (1979) 133–142;

TRANSIENT FIELD *g*-FACTOR MEASUREMENTS ON THE 2_1^+ STATES OF ^{32}S AND ^{34}S

P. C. ZALM †, A. HOLTHUIZEN, J. A. G. DE RAEDT and G. VAN MIDDELKOOP

Fysisch Laboratorium, Rijksuniversiteit, Utrecht, The Netherlands

Received 8 February 1978
(Revised 9 October 1978)

Abstract: Transient field integral precession measurements have been performed on the first-excited $J^\pi = 2^+$ states of ^{32}S and ^{34}S with the IMPAC technique on recoil into magnetized iron single-crystal frames. The results were analysed with an empirical parametrization of the field. This yields *g*-factors of $g = +0.47 \pm 0.09$ and $+0.50 \pm 0.08$ for ^{32}S and ^{34}S, respectively. In the present cases the influence of static magnetic hyperfine fields is negligible due to the short mean lives for ^{32}S and ^{34}S of 0.23 and 0.46 ps, respectively. Various complex model calculations yield *g*-factors in good agreement with experiment. Measured *g*-factors, including the present data, for light self-conjugate and neutron-excess $T_z = 1$ nuclei are also briefly discussed. The measured value of the *g*-factor for ^{32}S confirms the empirical description of the transient field.

E NUCLEAR REACTIONS ^{32}S(α, α′γ), $E = 8.25$ MeV; ^{34}S(α, α′γ), $E = 8.90$ MeV; measured $\alpha\gamma(\theta, B)$ in polarized Fe. ^{32,34}S levels deduced *g* for first 2^+ states. ^{34}S enriched target. IMPAC.

1. Introduction

The transient magnetic field experienced by a nucleus slowing down in magnetized Fe is currently explained by a transfer of polarized electrons from the ferromagnetic host into bound atomic s-shells of the moving nuclear ion [1–3]. It has been shown [2]) that this field can be parametrized as a (saw-tooth like) function of atomic number and as a (linear) function of recoil velocity of the moving ion. For nuclei with $Z \leq 14$ this parametrization yields a calibration which reproduces the measured field strength to within 5 %. It is expected that this calibration is still good for $Z < 20$. This enables one to perform *g*-factor measurements in this region on short-lived ($\tau = 0.1$–10 ps) excited states by the transient field implantation perturbed angular correlation (TF-IMPAC) technique. For states with lifetimes greater than the stopping time in Fe one can avoid contributions from the often not well-known static hyperfine fields by taking the ferromagnetic medium thin enough such that the nuclei recoil through

† Present address: Philips' Natuurkundig Laboratorium, Eindhoven, The Netherlands.

NUCLEAR INSTRUMENTS AND METHODS 161 (1979) 265-272 ; © NORTH-HOLLAND PUBLISHING CO.

THE USE OF SINGLE-CRYSTAL IRON FRAMES IN TRANSIENT FIELD MEASUREMENTS

P. C. ZALM*, J. VAN DER LAAN and G. VAN MIDDELKOOP

Fysisch Laboratorium, Rijksuniversiteit Utrecht, P.O. Box 80.000, 3508 TA Utrecht, The Netherlands

Received 3 January 1979

Single-crystal Fe frames have been investigated for use as a ferromagnetic backing in transient magnetic field experiments. For this purpose the surface magnetization as a function of applied magnetic field has been determined with the magneto-optical Kerr effect. The frames, which have two sides parallel to the ⟨100⟩ crystal axis, can be fully magnetized at low external fields such that fringing fields are negligibly small. These single-crystal Fe backings have been used in several transient magnetic field experiments. Comparison of the measured precession angles with previous results, obtained in polycrystalline Fe foils at high external magnetic fields, shows that the single-crystal backings are satisfactory. After extended periods of heavy-ion bombardment the crystals exhibited no radiation damage effects. The absence of fringing fields leads to a reduction of a factor of four in the measuring time for transient field experiments.

1. Introduction

The strong transient magnetic field is a powerful tool for measuring magnetic dipole moments of short-lived ($\tau_m = 0.1$–10 ps) excited nuclear states. In the transient field implantation perturbed angular correlation (TF–IMPAC) method[1,2]) excited and aligned nuclei, produced by a nuclear reaction, recoil into a (fully) magnetized ferromagnetic medium. During the slowing down the nucleus experiences the strong transient magnetic field[3]), which through the interaction with the nuclear magnetic moment causes the spin of the excited state to precess. This precession is observed as a rotation of the angular distribution of the γ-rays emitted in the decay of this state. The measured rotation is an integral over the slowing-down history weighted by the nuclear decay probability. Once the calibration of these dynamic fields as a function of recoil velocity and atomic number of the moving ion is known, the g-factor of the excited state can be extracted from the observed precession. The field calibration has been discussed elsewhere[3]), at least for ions with atomic number $Z \lesssim 20$. In the present paper we focus our attention on experimental procedures only.

In TF–IMPAC experiments the penetration depth of the recoiling ions in the ferromagnetic backing is typically only 1–5 μm. It is therefore of considerable importance to know the surface magnetization of these backings since the transient field is proportional to the degree of magnetization. In most transient field experiments polycrystalline Fe target backings have been used. As has been shown[4]) there may be a striking difference between the surface and bulk magnetization at low magnetizing fields. This phenomenon, a distinctive lag in the surface magnetization, is probably due to demagnetizing fields near the surface. For full surface magnetization external fields of the order of 0.1 T are necessary. This inevitably causes a non-negligible fringing field near the target, which has the following effects. Firstly the beam of incoming particles is bent in the fringing field, which turns the reference axis for the γ-ray angular distribution. Secondly, since γ-rays are always detected in coincidence with outgoing reaction particles at an average angle of 180° to the beam direction, the real mean detection angle is different from 180°. This off-axial detection causes a change in the magnetic substate populations of the nuclear state which is also observed as a rotation of the angular correlation[2]). The result of both effects, called the beam-bending effect, is not calculable except for pure Coulomb excitation. It must therefore be measured independently with a non-ferromagnetic backing and subtracted from the total effect in order to obtain the real transient field rotation angle. Since the experimental conditions for the two measurements should be identical, the resulting experimental errors are approximately equal. Hence the total measuring time required for a given error in the net rotation is four times as long as it would be in the absence of the beam-bending effect.

In the present paper we present a method to circumvent these problems by using a single-crystal iron frame as a target backing. Preliminary results

* Present address: Philips' Natuurkundig Laboratorium, Eindhoven, The Netherlands.

Inst. Phys. Conf. Ser. No. 49: Chapter 1

Nuclear structure calculations in the fp shell

P W M Glaudemans
Fysisch Laboratorium, Rijksuniversiteit Utrecht, Princetonplein 5, 3508 TA Utrecht, The Netherlands

Abstract. Detailed shell-model calculations have been performed for nuclei in the middle of the fp shell. Examples of the results obtained with slightly modified Kuo–Brown matrix elements and the surface delta interaction are presented. With the modified Kuo–Brown interaction, very good agreement is obtained for ^{56}Fe. The surface delta interaction is superior when the $f_{5/2}$ orbit plays a significant role.

1. Introduction

The purpose of this paper is to demonstrate the feasibility of performing large-scale shell-model calculations to obtain a detailed description of nuclei in the middle of the fp shell. The present calculations are concentrated on spectra (including those of high-spin states), spectroscopic factors, electromagnetic transition rates and moments and log ft values. Since several nuclei in this mass region exhibit collective features, a comparison between the shell model and the collective model may be possible. As a start, the lighter isotopes of Ni, Co and Fe have been investigated.

The two main problems, as in any shell-model calculation, are the choice of the most appropriate configuration space and the corresponding effective one- and two-body interaction. These topics are discussed in §§2 and 3. Examples of the results obtained so far are presented in §4.

2. The model space

Let us consider the Ni isotopes as an example. The simplest shell model for a description of, for example, the lower states of $^{57}_{28}Ni_{29}$ and $^{58}_{28}Ni_{30}$ is to consider these states as formed by an inert $^{56}_{28}Ni_{28}$ core plus one and two particles, respectively. Excitation energies and spectroscopic factors can then be rather well accounted for, but a reasonable description of electromagnetic properties requires the use of an appreciable renormalisation of the M1 and E2 single-particle matrix elements (Koops 1978). It is shown that, by the inclusion of single-particle core excitations, the electromagnetic properties can be reproduced without renormalisation of the M1 operator and with much smaller effective charges. The configuration space employed can be represented by

$$(p_{3/2}f_{5/2}p_{1/2})^m + f_{7/2}^{-1}(p_{3/2}f_{5/2}p_{1/2})^{m+1}$$

with $m = 1$ and 2 for ^{57}Ni and ^{58}Ni, respectively.

The results for ^{57}Ni are displayed in figure 1. For the two-body interaction, the surface delta interaction (SDI) has been taken. The strength parameters and single-particle

Z. Physik A 293, 327–335 (1979)

Zeitschrift
für Physik A

The Influence of $f_{7/2}$ Hole Configurations on Properties of $^{57-59}$Ni

A.G.M. van Hees, P.W.M. Glaudemans and B.C. Metsch
Fysisch Laboratorium, Rijksuniversiteit Utrecht, Utrecht, The Netherlands

Received August 7, 1979

Shell-model calculations have been performed on $^{57-59}$Ni. All configurations with one hole in the $f_{7/2}$ orbit have been included exactly. The results of a newly proposed approximation method are in good agreement with those of the exact calculations, when applied to the predominant zero-hole states. The experimental results are compared with those of the realistic Kuo-Brown interaction and the schematic Surface Delta Interaction. The role of the $f_{5/2}$ orbit differs significantly for these two interactions. The results show that $f_{7/2}$ hole contributions strongly improve the description of the Ni isotopes.

1. Introduction

In this paper we present the first results of a systematic shell-model investigation of nuclei in the mass region around ^{56}Ni. In these studies the configuration space is taken as large as feasible with available computer facilities.

The present investigation of $^{57-59}$Ni is concentrated on (i) a critical evaluation of two well-known sets of two-body matrix elements i.e. those obtained from the realistic Kuo-Brown interaction (KB) and from the schematic Surface Delta Interaction (SDI), (ii) a detailed test of the proposed approximation method, which allows one to take into account effects of a configuration space too large to be treated exactly, (iii) a study of the effects of the break-up of the ^{56}Ni core.

The Ni isotopes have previously [1, 2] been treated in the shell model in a configuration space with a doubly closed ^{56}Ni core, and the active neutrons distributed over the $2p_{3/2}$, $1f_{5/2}$ and $2p_{1/2}$ orbits. Within this configuration space and with two-body matrix elements derived from the Surface Delta Interaction [3] the spectra and single-particle spectroscopic factors can be well described. For a reasonable reproduction of electromagnetic properties the introduction of strongly modified transition operators was required, however. An optimalisation of the two-body interaction by means of a least-squares fit to excitation energies did not further improve the electromagnetic properties [4]. The large renormalisations of the transition operators, needed when one assumes a closed ^{56}Ni core, indicate that this model space is much too restricted. In the present paper the effects due to an extension of the configuration space are investigated. Such an extension is achieved by also taking into account states with one hole in the $1f_{7/2}$ orbit. The dimensions of the matrices involved increase considerably. Hence, it is desirable to develop a method which reduces the computer time needed for the construction and diagonalisation of large matrices. An approximation method for this purpose is described in Sect. 2.2. For states with a zero-hole part dominating the wave function this method is tested by comparing its results with those of the exact calculation (see Sect. 3.1).

The complete zero-hole plus one-hole calculations have been performed both with SDI and Kuo-Brown matrix elements in order to investigate the influence of the two-body interaction on the results (see Sect. 3.2). The states with a predominant one-hole character are discussed separately in Sect. 4. Some remarkable discrepancies between the results obtained with SDI and Kuo-Brown matrix elements can sometimes be attributed to the different role of the $1f_{5/2}$ orbit in the two interactions (see Sect. 5).

0340-2193/79/0293/0327/$01.80

CENTRAL AND NONCENTRAL COMPONENTS OF THE PREEDOM–WILDENTHAL INTERACTION

G.A. TIMMER, R. VAN DER HEYDEN and B.C. METSCH
Fysisch Laboratorium, Rijksuniversiteit Utrecht, The Netherlands

and

K. KLINGENBECK
Institut für Theoretische Physik, Universität Erlangen-Nürnberg, Erlangen, West Germany

Received 17 October 1978

The influence of the various components of the Preedom–Wildenthal interaction – viz., central, tensor, spin–orbit (LS) and antisymmetric spin–orbit (ALS) – on properties of $A = 20,21$ nuclei is investigated. The effects of the LS and ALS components on the one hand and of the central and tensor components on the other hand are found to be very similar. It turns out to be possible to remove the ALS component in favour of an enhanced LS component without spoiling the agreement with experiment.

Following the techniques described in refs. [1–3] one can write a given effective two-body interaction as a sum of central (C), tensor (T), spin–orbit (LS) and antisymmetric spin–orbit (ALS) components. In order to discern the influence of the various components, the interaction $V = \Sigma V_i$ is written here as $\Sigma \lambda_i V_i$ with λ_i denoting strength parameters that are to be varied (i = C, T, LS, ALS). In the calculations to be described below the Preedom–Wildenthal (PW) interaction [4] was employed, i.e. $V_{PW} = \Sigma V_i$. No separate strength parameters for the $T = 0$ and $T = 1$ channels were considered.

In a first step the energy spectra and electromagnetic properties of $A = 20$ and $A = 21$ nuclei were calculated as a function of the strength parameters. A rather detailed account along these lines has been given in ref. [2] for the case of ^{24}Mg. In ref. [2] it was stressed that a large enhancement of the ALS strength ($\lambda_{ALS} \approx 5$) of the Kuo–Brown interaction in a SU(3) truncated model space led to a marked improvement in the description of ^{24}Mg. Our calculation on $A = 20$ and $A = 21$ nuclei led to a different picture. The principal result was a remarkable coherence in the effects of varying λ_{LS} or λ_{ALS} on the one hand and λ_C or λ_T on the other hand. In fig. 1 this is illustrated for magnetic moments. The values in fig. 1 were obtained upon variation of one strength parameter at a time, while the others were fixed at unity. With relatively few exceptions the same clear trends persisted for other quantities (E2 and M1 transition rates, quadrupole moments, wave function overlaps etc.) as well. Only for energies, C and T showed an opposite behaviour, see fig. 2. The low-lying states of ^{20}Ne are of a rather pure $S = 0$ nature, henceforth preventing a sizable first-order effect of the noncentral components. Nevertheless, the trends mentioned before emerged in this case also.

The coherence of the LS and ALS effects suggests that it might be possible to remove the ALS component in the PW interaction in favour of an enhanced LS component. Although there have been given some explanations [2,3] for the presence of an ALS term, it has not yet been possible to justify the large contributions of the ALS term to an effective interaction. Hence, in our opinion it is worthwhile to postpone as long as possible the introduction of such a term which is virtually absent in the free nucleon–nucleon interaction.

A STATISTICAL STUDY OF SHELL-MODEL EIGENVECTORS

J.J.M. VERBAARSCHOT and P.J. BRUSSAARD
Fysisch Laboratorium, Rijksuniversiteit Utrecht, 3508 TA Utrecht, The Netherlands

Received 21 November 1978
Revised manuscript received 23 May 1979

The components of shell-model eigenvectors show a non-gaussian distribution that can be derived by the use of the Porter–Thomas proposition.

In nuclear shell-model calculations one is confronted with increasing dimensionalities of the configuration spaces. It makes sense, therefore, to study the statistical properties of the eigenvectors of nuclear states. The distribution of the amplitudes of the eigenvector components of a large-scale shell-model hamiltonian shows a predominance of the small amplitudes.

The distribution is not gaussian, however, but more complicated. In this paper we shall derive an explicit expression for the amplitude distribution from three statistical assumptions. No parameters are to be fitted for the final expression. Several papers (e.g. ref. [1]) have been devoted to studies of the gaussian orthogonal ensemble of matrices. Here, however, we do not consider an ensemble of hamiltonians, but rather study the eigenvalues and eigenvectors of one hamiltonian.

Let the eigenvectors ψ_i of the hamiltonian, H, be expanded in the basis $\{\phi_\alpha\}$ $(\alpha = 1, 2, ..., N)$:

$$\psi_i = \sum_{\alpha=1}^{N} c_{\alpha i}\phi_\alpha , \quad i = 1, ..., N . \tag{1}$$

The two-body interaction used to construct the hamiltonian for our calculations was the MSDI [2]. The basis states ϕ_α were taken to span the full sd-shell. For the $J^\pi = 1/2^+$ states of ^{25}Mg this leads to a dimension 1434 and for the $J^\pi = 1^+$ states of ^{22}Na to a dimension 243. For a fixed eigenvector we can plot the values of the coefficients $|c_{\alpha i}| = |\langle\phi_\alpha|\psi_i\rangle|$ versus the values of the diagonal matrix elements $H_{\alpha\alpha} = \langle\phi_\alpha|H|\phi_\alpha\rangle$. In fig. 1 such a plot is shown for the lowest $J^\pi = 1^+$ eigenstate of ^{22}Na. One observes a *secular* variation $|c_{\alpha i}|$ as a function of $H_{\alpha\alpha}$ (solid line) and fluctuations of the actual values of the amplitudes $|c_{\alpha i}|$ around the average.

These fluctuations will be described by the Porter–Thomas proposition [3] that the coefficients $c_{\alpha i}$ locally, i.e. for some small neighbourhood of $H_{\alpha\alpha}$, show a normal distribution with zero mean. This gaussian behaviour implies that the variance is proportional to the secular value

$$\overline{\langle\phi_\alpha|\psi_i\rangle^2} = (\pi/2)\overline{|\langle\phi_\alpha|\psi_i\rangle|}^2 . \tag{2}$$

We assume that the diagonal matrix elements

$$H_{\alpha\alpha} \equiv \langle\phi_\alpha|H|\phi_\alpha\rangle , \quad (\alpha = 1, 2, ..., N) , \tag{3}$$

possess a gaussian distribution

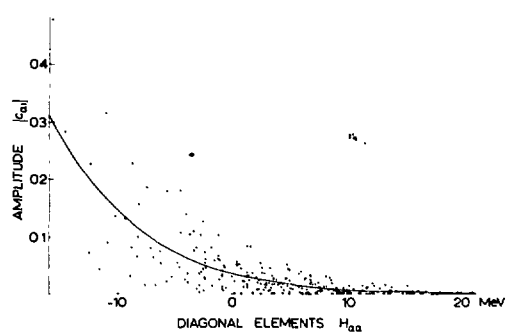

Fig. 1. The amplitudes $|\langle\phi_\alpha|\psi_i\rangle|$ versus the diagonal elements $\langle\phi_\alpha|H|\phi_\alpha\rangle$. The solid line is the secular variation ρ_I.

Proc. AMCO 6 (1979); Plenum Press

GAMMA-RAY ENERGY CALIBRATION STANDARDS

C. van der Leun*, R.G. Helmer** and P.H.M. Van Assche***

Task group of the IUPAP Commission on Atomic Masses and Fundamental Constants

INTRODUCTION

The task group on gamma-ray calibration standards was established in 1972 by the IUPAP Commission on Atomic Masses and Fundamental Constants. Its task is the production, recommendation and publication of a consistent set of calibration standards for use in gamma-ray spectroscopy.

The present paper is the first official report of the task group. It presents a consistent set of gamma-ray energies, all with uncertainties of at most 10 ppm. The energies, in the range E_γ = 60 - 6100 keV, are based on the value[1] E_γ = 411 804.4 $\pm$ 1.1 eV for the gamma-ray from the decay of ^{198}Au. The highest gamma-ray energy listed, that of the 6129 keV line in ^{16}O, can be compared with an energy measurement[2] based on a mass-doublet scale.

A more detailed account of the activities of the task group will be published in the near future[3].

GAMMA-RAY ENERGY SCALES

Shortly after the establishment of the task group it became apparent that two completely different experiments were underway, that would both provide a definition of the gamma-ray energy scale

* Fysisch Laboratorium, Rijksuniversiteit, Princetonplein 5, 3508 TA Utrecht, The Netherlands; task group chairman.

** EG&G Idaho, Idaho Falls, Idaho, USA; work performed under the auspices of the U.S. Department of Energy.

*** SCK-CEN, Nuclear Energy Centre, Mol, Belgium.

ATOMIC DATA AND NUCLEAR DATA TABLES 23, 3–61 (1979)

STRENGTHS OF GAMMA-RAY TRANSITIONS IN A = 6–44 NUCLEI (III)

P. M. ENDT

Fysisch Laboratorium, Rijksuniversiteit Utrecht
Princetonplein 5, 3508 TA Utrecht, The Netherlands

The present tables list the strengths (in Weisskopf units) of over 2400 γ-ray transitions in A = 6–44 nuclei, classified according to character (electric or magnetic, multipolarity, isospin forbiddenness). Selected transitions from unbound states are included. The strengths for isovector $E1$ and $M1$ transitions ($E1_{IV}$ and $M1_{IV}$) show a marked decrease with A. Strengths depend very little on the excitation energy of the initial state. The new data incorporated in the tables have not given rise to changes in the recommended upper limits (RUL) for γ-ray strengths presently in use. The only exception is the (spectroscopically unimportant) RUL for $E1_{IV}$ transitions which should be raised from 0.1 to 0.3 W.u. for A = 6–20 nuclei.

0092-640X/79/010003-59$02.00/0

Newsletter Int. Target Development Society (July 1979)

9

A. MICHIELSEN

FYSISCH LABORATORIUM DER RIJKSUNIVERSITEIT UTRECHT

PRINCETONPLEIN 4, UTRECHT

THE NETHERLANDS

Preparation of Red-Phosphorus Targets

The preparation of thick phosphorus targets by means of boat evaporation is a difficult process, which contaminates the evaporation unit.

Therefore, we prepared these targets with a heavy ion sputtering unit (Danfysik, Denmark). Lumps of red-phosphorus (purity 99,999%) are powdered in an argon atmosphere. The carbon crucible (see figure) is filled with the red-phosphorus powder. The powder is pressed into the hole in the middle of the crucible with a glass rod. This is done to prevent the material from jumping out during the sputtering process. The crucible and the substrate holder are put into the bell-jar. The distance between the middle of the crucible and the substrate is 15 mm.

As substrates, gold foils with a thickness of 20-300 μm are used. The material to be sputtered is bombarded by an argon- or xenon-beam, delivered by a duoplasmatron ion source. In the case of a xenon beam, the sputtering process goes faster, but the process is more difficult to regulate than with an argon beam.

The prepared phosphorus targets had a thickness of 50 to 500 $\mu g/cm^2$. To obtain target thicknesses of the order of 500 $\mu g/cm^2$, it is necessary to fill the crucible three times with red-phosphorus. The thickness of the targets is measured by weighing them on a micro-balance. The accuracy is 1-2 $\mu g/cm^2$.

NUCLEAR INSTRUMENTS AND METHODS 163 (1979) 309-311; © NORTH-HOLLAND PUBLISHING CO.

AN IMPROVED ION SOURCE EXTRACTION SYSTEM OF A 3 MV VAN DE GRAAFF ACCELERATOR

A. VERMEER and A. J. VEENENBOS

Fysisch Laboratorium, Rijksuniversiteit, P.O. Box 80.000, Utrecht, The Netherlands

Received 26 February 1979

The proton beam current available from our KN 3000 Van de Graaff accelerator has been more than doubled by the installation of a newly designed focussing electrode.

1. Introduction

The HVEC KN 3000 Van de Graaff generator in Utrecht provided stable proton beam currents of up to about 90 μA. Higher beam-current settings caused the beam to jump to another "mode", in which the beam could not be adequately focussed. Fig. 1 gives an illustration of this phenomenon measured with a beam profile monitor, placed at the position of the entry slits of the analysing magnet. A well focussed proton beam is observed for beam currents up to 90 μA (lower beam). A small change in the settings of the control knobs leads to a badly focussed beam of 120 μA (upper beam), that can hardly be manipulated by the ion-source controls, such as the gas- and magnet controls. The ion source had to be restarted from zero current to get back the well-focussed mode. During these measurements the generator was provided with a HVEC-C-SO-173 ion source, with a pyrex bottle and a stainless steel lined aluminum canal (length = 12 mm, $\emptyset$ = 2.1 mm). According to the specifications the source can deliver proton beams of more than 1 mA.

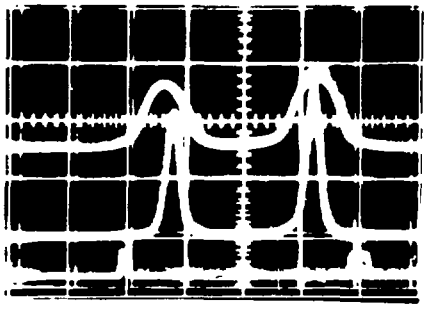

Fig. 1. Profiles of the proton beam measured with a beam-profile monitor. Lower beam: a well-focussed proton beam of 90 μA. Upper beam: a badly focussed proton beam of 120 μA. The distance between the two markers is 38 mm.

Since high beam currents are essential for several nuclear structure experiments, the limitations of the beam current were investigated. Because the observed phenomena strongly suggested shortcomings in the functioning of the ion source and extraction system, this part of the accelerator was investigated in more detail.

2. The ion source system

The operation of the ion source and the extraction system was studied at the accelerator with rolled-off tank. The beam current of the ion source can then be measured by using the accelerator tube as a Faraday cup by electrically connecting all the electrodes. With this set-up it was found that at higher beam-current settings, the measured beam current was only a small fraction of the current on the focussing electrode. This caused a heavy loading of the focus power supply and impeded the functioning of the focussing electrode. Lowering the internal resistance of the focus power supply from 5 MΩ to 100 kΩ and increasing the rectifiers from 5 to 20 mA gave only a small improvement. The mentioned phenomena clearly show that at higher beam-current settings a gas discharge appeared between the exit of the source and the focussing electrode. This caused a blowing-up of the beam and partly a short-circuiting of the focussing electrode.

The vacuum at the focussing electrode, which is rather critical, is obtained by pumping via the accelerator tube. The conductance of the accelerating tube is rather low; for hydrogen between 30 and 40 l/s, depending on the pressure. At the source end of the tube the focussing electrode is mounted on a metal plate. The pressure at the extraction system of the ion source is obtained by pumping through the canal (length = 87 mm, $\emptyset$ = 14 mm) in the focussing electrode (see fig. 2, lower half). This

8. PAPERS IN PRESS

Accepted for publication in Nucl. Instr.

IMPROVEMENT OF THE PERFORMANCE OF A COMPTON-SUPPRESSION SPECTROMETER BY MINIMIZING THE DEAD LAYER OF THE CENTRAL Ge DETECTOR

H.J.M. Aarts, G.A.P. Engelbertink, C.J. van der Poel,
D.E.C. Scherpenzeel and H.F.R. Arciszewski

Abstract: The performance of a Compton-suppression spectrometer is investigated for two different Ge crystals as central detector; a 126 cm^3 Ge(Li) with a dead layer of 1.0 mm and a 90 cm^3 HPGe with a dead layer of 0.22 mm. The thin dead layer HPGe gives a 32% improvement in the overall Compton suppression. Predictions of the influence of the dead-layer thickness by means of Monte Carlo calculations are in good agreement. The spectrometer is further tested with radioactive sources of ^{88}Y and ^{152}Eu and the in-beam reaction ^{24}Mg + (45 MeV) ^{16}O.

Submitted for publication in Nucl. Phys.

COINCIDENT HIGH-VELOCITY DSA LIFETIME MEASUREMENTS ON EXCITED STATES OF Si ISOTOPES, AND STOPPING POWER INVESTIGATIONS

D.E.C. Scherpenzeel, G.A.P. Engelbertink, H.J.M. Aarts,
C.J. van der Poel and H.F.R. Arciszewski

Abstract: Mean lives of low-lying states of ^{28}Si, ^{29}Si and ^{30}Si have been measured with the coincident high-velocity DSA method by ^{28}Si bombardment of ^{2}H, ^{3}H and ^{4}He targets. The recoils with an initial velocity of about 4.8% are slowed down in Mg, Cu, Ag and Au. The emitted γ-ray Doppler patterns are observed with a Ge(Li) detector at $\theta_\gamma = 0^\circ$ in coincidence with outgoing particles. The results are: ^{28}Si, τ_m(1.78 MeV) = 688 ± 26 fs; ^{29}Si, 420 ± 15, 442 ± 14, 26.6 ± 1.6, 46 ± 3 and 3740 ± 190 fs for states at 1.27, 2.03, 2.43, 3.07 and 3.62 MeV, respectively; ^{30}Si, τ_m(2.24 MeV) = 358 ± 18 fs. The deduced transition strengths are compared with shell-model calculations. Stopping powers obtained from Ziegler's effective charge parametrization are compared to experimental data. The usual DSA procedure is also reversed in the sense that a well-established mean life is used to deduce the electronic stopping power for Si ions in Mg. The result found is verified by other DSA measurements.

Accepted for publication in Hyperfine Int.

THE TRANSIENT MAGNETIC FIELD AT LOW VELOCITIES

J.A.G. De Raedt , A. Holthuizen, A.J. Rutten, W.A. Sterrenburg
and G. van Middelkoop

Abstract: A method has been developed, based on a Doppler-shift measurement, for determining the transient magnetic field effect as a function of the actual velocity v of the recoiling ion without varying the initial velocity. This method has been applied to the first-excited state of ^{28}Si recoiling into iron at an initial velocity of $v_i = 2.0\ v_o$ ($v_o = c/137$). The data are consistent with a field strength proportional to v down to $v = 0.2\ v_o$. A simple model is introduced which might explain the observed v-dependence but fails to account for the known Z_1 dependence.

Accepted for publication in Nucl. Phys.

MEASUREMENT OF THE g-FACTOR AND LIFETIME OF THE FIRST-EXCITED STATE OF ^{20}O

A.J. Rutten, A. Holthuizen, J.A.G. De Raedt ,
W.A. Sterrenburg and G. van Middelkoop

Abstract: The g-factor and mean lifetime of the first-excited 2^+ state at 1.67 MeV in ^{20}O have been determined by means of a plunger set-up. The state was populated by the ^{3}H(^{18}O,pγ)^{20}O reaction at $E(^{18}O) = 24.5$ MeV. The analysis of p-γ anisotropies as a function of flight path of the recoiling ion in vacuum leads to a value for the g-factor of $|g| = 0.352 \pm 0.015$ and to a mean life of $\tau = 10.7 \pm 0.4$ ps.

Accepted for publication in Nucl. Instr.

A NEGATIVE ION SOURCE FOR ALKALI IONS

A. VERMEER and N.A. VAN ZWOL

Abstract: An ion source is described which delivers negative alkali ions With this source, which consists of a duoplasmatron and a charge exchange canal with alkali vapour, negative Li, Na and K ions are produced. The oven in which alkali metals are evaporated can reach temperatures up to 575 °C.

Accepted for publication in Nucl. Instr.

THE CONDUCTANCE FOR GAS FLOW OF AN ACCELERATING TUBE

A. Vermeer and N.A. van Zwol

Summary: Measurements of the conductance in the molecular flow region of accelerating tubes of an EN tandem are given and discussed. These measurements have been done on both straight and inclined field tubes. A theoretical model is constructed by means of which the conductance of an accelerating tube can be calculated. The calculated values of the conductance turn out to be in a good agreement with the measured ones.

Accepted for publication in Z. Physik

The Shell Model and Collective Structures in ^{54,55,56}Fe

R. Vennink
FOM-ECN Nuclear Structure Group, Netherlands Energy Research Foundation, Petten, The Netherlands

P.W.M. Glaudemans
Fysisch Laboratorium, Rijksuniversiteit, Utrecht, The Netherlands

Received September 18, Revised Version November 5, 1979

Extensive shell-model calculations have been performed on ^{54,55,56}Fe. The results obtained in a model space with two and with up to three $f_{7/2}$ holes in the ^{56}Ni core are compared with experiment. The Surface Delta Interaction (SDI) and the Kuo Brown interaction (KB) have been used to calculate energy levels, spectroscopic factors and electromagnetic properties resulting especially for ^{56}Fe in a remarkably good agreement with experiment. Admixtures of three-hole components in the wave functions are significant and increase with mass number. Properties of high-spin states with $J \leqq 15$ are discussed. Pronounced collective features derived microscopically are expected in ^{56}Fe. Finally some suggestions for interesting experiments are given.

Accepted for publication in Nucl. Phys.

INVESTIGATION OF THE ^{56}Fe(n,γ)^{57}Fe AND ^{58}Fe(n,γ)^{59}Fe REACTIONS

R. Vennink and J. Kopecky

FOM-ECN Nuclear Structure Group, Netherlands Energy Research Foundation

Westerduinweg 3, 1755 ZG Petten, The Netherlands

P.M. Endt and P.W.M. Glaudemans

Fysisch Laboratorium, Rijksuniversiteit Utrecht,

Princetonplein 5, 3508 TA Utrecht, The Netherlands

Submitted for publication in Nucl. Phys.

SPECTROSCOPIC PROPERTIES AND COLLECTIVE STRUCTURE FROM A SHELL-MODEL DESCRIPTION OF A = 53 NUCLEI

B.C. METSCH and P.W.M. GLAUDEMANS

Abstract: A shell-model calculation on the structure of negative-parity states in A = 53 isobars is presented. Results on spectra, electromagnetic transition rates and moments, β-decay, high-multipolarity transitions and spectroscopic factors obtained with a modified Kuo-Brown force and with the Surface Delta Interaction are compared with experiment. The measured E6, M5 and E4 transition strengths in ^{53}Fe can be rather well explained. The existence of a pure K = 1/2 band in ^{53}Fe is suggested by the microscopic calculation. Recently measured excitation energies of high-spin states in ^{53}Mn are in excellent agreement with the theory.

Accepted for publication in Phys. Lett.

A MICROSCOPIC CLASSIFICATION OF HIGH-SPIN STATES IN ^{56}Fe

P.W.M. Glaudemans

Fysisch Laboratorium, Rijksuniversiteit, Utrecht, The Netherlands

and

R. Vennink

FOM-ECN Nuclear Structure Group, Netherlands Energy Research Foundation, Petten, The Netherlands

Abstract

A large-scale shell-model calculation on ^{56}Fe including positive-parity states with spins up to J = 15 shows that several states in the yrast region are of a particular nature. These states can be arranged in groups of which the gamma decay and quadrupole moments show a collective behaviour. The signature of each group is the $f_{7/2}$ hole structure which is coupled to its maximum angular momentum. The level density above the yrast region turns out to be largely independent of J.

Accepted for publication in Atomic Data and Nuclear Data Tables

RECOMMENDED STANDARDS FOR GAMMA-RAY ENERGY CALIBRATION (1979)

R.G. HELMER , P.H.M. VAN ASSCHE and C. VAN DER LEUN

Task group of the IUPAP Commission on

Atomic Masses and Fundamental Constants

A consistent set of γ-ray energies, all with uncertainties of at most 10 ppm, is recommended for use in the energy calibration of γ-ray spectra. Almost all γ-rays listed are from commercially available sources. The half-lives of the isotopes selected are generally at least 30 days.

The γ-ray energies, in the range E_γ = 60 - 6100 keV, are all based on the value of 411 804.4 ± 1.1 eV for the γ-ray from the decay of ^{198}Au. The energy of the 6129 keV line in ^{16}O, which is the γ-ray with the highest energy of the present set, has also been measured relative to another standard; the two values are consistent.

Accepted for publication in Atomic Data and Nuclear Data Tables

STRENGTHS OF GAMMA-RAY TRANSITIONS IN A = 45-90 NUCLEI

P.M. Endt

The present tables list the strengths (in Weisskopf units) of over 1200 transitions in A = 45-90 nuclei, classified according to character (electric or magnetic, multipolarity).

It appears that E1, M1 and M2 transitions are weaker than in the A = 6-44 region, whereas E2 transitions are slightly stronger.

The following recommended upper limits for the A = 45-90 region can be deduced from the data: 0.01, 300, 100 and 100 W.u. for E1, E2, E3 and E4, and 3, 1, 10 and 30 W.u. for M1, M2, M3 and M4, respectively.

To be published in Nucl. Phys.

ERRATA AND ADDENDA

P.M. ENDT and C. VAN DER LEUN,
Energy levels of A = 21-44 nuclei (VI),
Nucl. Phys. A310 (1978) 1.

9. CONFERENCE CONTRIBUTIONS

DPG + NNV MEETING, Gent, March 1978

- H.J.M. Aarts, G.A.P. Engelbertink, C.J. van der Poel and D.E.C. Scherpenzeel,
  "Coincident high-velocity lifetime measurements with the $^{4}He(^{28}Si,\alpha\gamma)^{28}Si$ and $^{2}H(^{28}Si,p\gamma)^{29}Si$ reactions".
- H.J.M. Aarts, G.A.P. Engelbertink, C.J. van der Poel and D.E.C. Scherpenzeel,
  "High-spin yrast levels of ^{38}Ar".
- K. Abrahams, J. de Boer, P.P.J. Delhey, J.B.M. de Haas and J. Kopecky,
  "Capture of polarized neutrons and the study of 2p states".
- C. Alderliesten, P.F.A. Alkemade, J.A. van Nie, P. de Wit and C. van der Leun,
  "Precision measurements of high-energy γ-rays".
- P.H.M. van Assche, R.G. Helmer and C. van der Leun,
  "Evaluation of γ-ray energies for calibration".
- J.R. Balder,
  "Gamma-gamma angular correlation measurements after thermal neutron capture".
- A. Becker, J.A.G. de Raedt, A. Holthuizen, A.J. Rutten, G. van Middelkoop and R. Kalish,
  "Transient magnetic fields on light nuclei in gadolinium".
- R.J. Elsenaar, E.L. Bakkum, J.C.J. Kock, H. van der Vlist, F. Zijderhand and C. van der Leun,
  "A discrepancy in the attosecond lifetimes deduced from (e,e') and (γ,γ) experiments".
- P.M. Endt,
  "Strengths of γ-ray transitions in A = 6-44 nuclei".
- P.W.M. Glaudemans, A.G.M. van Hees, B.C. Metsch and D. Zwarts,
  "Shell-model calculations in the middle of the fp shell".
- P.W.M. Glaudemans, A.G.M. van Hees, B.C. Metsch and D. Zwarts,
  "On the structure of light Co-isotopes".
- G.J.L. Nooren, S. van der Meij, F.M. Bloemen and C. van der Leun,
  "The reaction $^{36}S(p,\gamma)^{37}Cl$".
- J.A.G. de Raedt, A. Holthuizen, A.J. Rutten, W.A. Sterrenburg and G. van Middelkoop,
  "Recoil-distance measurements of the g-factor and lifetime for $^{20}O(2_1^+)$".
- J.J.M. Verbaarschot and P.J. Brussaard,
  "A statistical study of shell-model eigenvectors".
- A. Vermeer and A.J. Veenenbos,
  "An improved ion source extraction system of a 3 MV Van de Graaff generator".

CONFERENCE on MEDIUM-HEAVY NUCLEI, Rhodos, May 1978

- P.W.M. Glaudemans,
  "Nuclear Structure calculations in the fp shell".

CONFERENCE on ATOMIC MASSES and FUNDAMENTAL CONSTANTS, East Lansing, September 1979

- C. van der Leun, R.G. Helmer and P.H.M. van Assche,
  "Recommended γ-ray calibration energies".

DUTCH PHYSICAL SOCIETY, FALL MEETING, Petten, October 1978

- C. Alderliesten, P.F. Alkemade, P. de Wit and C. van der Leun,
  "Precise measurements of γ-ray energies".
- A. Becker, A. Holthuizen, R. Kalish, A.J. Rutten and G. van Middelkoop,
  "Transient field scaling and g-factor measurements".
- P.M. Endt,
  "Strengths of γ-transitions in the A = 45-90 region".
- P.W.M. Glaudemans and R. Vennink,
  "Collective structure in ^{56}Fe resulting from a microscopic calculation".
- P.M.J. Hoppenbrouwers and C. van der Leun,
  "The reaction ^{54}Fe(p,γ)^{55}Co".
- C. van der Leun, R.G. Helmer and P.H.M. van Assche,
  "Recommended standards for γ-ray energy calibration (1979)".
- B.C. Metsch and P.W.M. Glaudemans,
  "Calculation of the M8 strength distribution in some fp shell nuclei".
- G.J.L. Nooren, F.M. Bloemen, A. Buijs, S. van der Meij, A.P. Riethoff and C. van der Leun,
  "Resonances in ^{36}S(p,γ)^{37}Cl".
- C.J. van der Poel, H.J.M. Aarts, G.A.P. Engelbertink and D.E.C. Scherpenzeel,
  "High-spin states of ^{34}Cl".
- A. Vermeer and N.A. van Zwol,
  "A duoplasmatron for heavy ions".

WORKSHOP on GAMMA-RAY SPECTROSCOPY, Beekbergen, November 1979

- P.W.M. Glaudemans,
  "Collective effects in shell-model calculations".
- C.J. van der Poel,
  "High-spin states in ^{34}Cl".

10. OTHER LECTURES BY STAFF MEMBERS

P.W.M. Glaudemans

"Perspectieven voor het kernstructuuronderzoek in Utrecht"
Veldhoven, 11 May

"Nuclear structure in the fp shell"
Darmstadt, 13 December

C. van der Leun

"Measurements of very short lifetimes"
Edmonton, 11 September

G. van Middelkoop

"Zeer sterke magnetische stootvelden"
Enschede, 24 January

"Transient fields and g-factor measurements"
Duke University, 13 September, and East Lansing, 18 September

11. PH.D. THESIS

R. Vennink
"Investigation of some nuclei in the fp-shell-region"
23 April 1979